(12)

AFWAL-TR-82-4102

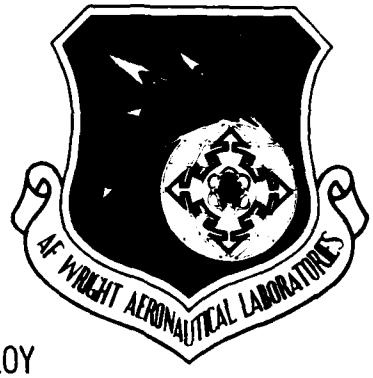

AD A130395

STATISTICS OF CRACK GROWTH OF A SUPERALLOY UNDER SUSTAINED LOAD

J. N. Yang
R. C. Donath

Metals Behavior Branch
Metals and Ceramics Division

December 1982

Final Report for Period January 1982 - June 1982

Approved for public release; distribution unlimited.

DTIC FILE COPY

MATERIALS LABORATORY
AIR FORCE WRIGHT AERONAUTICAL LABORATORIES
AIR FORCE SYSTEMS COMMAND
WRIGHT-PATTERSON AIR FORCE BASE, OHIO 45433

NOTICE

When Government drawings, specifications, or other data are used for any purpose other than in connection with a definitely related Government procurement operation, the United States Government thereby incurs no responsibility nor any obligation whatsoever; and the fact that the government may have formulated, furnished, or in any way supplied the said drawings, specifications, or other data, is not to be regarded by implication or otherwise as in any manner licensing the holder or any other person or corporation, or conveying any rights or permission to manufacture, use, or sell any patented invention that may in any way be related thereto.

This report has been reviewed by the Office of Public Affairs (ASD/PA) and is releasable to the National Technical Information Service (NTIS). At NTIS, it will be available to the general public, including foreign nations.

This technical report has been reviewed and is approved for publication.

R. C. Donath

R. C. DONATH, Project Engineer
Metals Behavior Branch
Metals and Ceramics Division

John P. Henderson

JOHN P. HENDERSON, Chief
Metals Behavior Branch
Metals and Ceramics Division

FOR THE COMMANDER

Lawrence N. Hjelm

LAWRENCE N. HJELM, Asst. Chief
Metals and Ceramics Division
Materials Laboratory

"If your address has changed, if you wish to be removed from our mailing list, or if the addressee is no longer employed by your organization please notify AFWAL/MLLN *,W-PAFB, OH 45433 to help us maintain a current mailing list".*

Copies of this report should not be returned unless return is required by security considerations, contractual obligations, or notice on a specific document.

UNCLASSIFIED

SECURITY CLASSIFICATION OF THIS PAGE (When Data Entered)

REPORT DOCUMENTATION PAGE		READ INSTRUCTIONS BEFORE COMPLETING FORM
1. REPORT NUMBER AFWAL-TR-82-4102	2. GOVT ACCESSION NO.	3. RECIPIENT'S CATALOG NUMBER
4. TITLE (and Subtitle) STATISTICS OF CRACK GROWTH OF A SUPERALLOY UNDER SUSTAINED LOAD		5. TYPE OF REPORT & PERIOD COVERED January 1982 - June 1982 6. PERFORMING ORG. REPORT NUMBER
7. AUTHOR(s) J. N. Yang and R. C. Donath		8. CONTRACT OR GRANT NUMBER(s)
9. PERFORMING ORGANIZATION NAME AND ADDRESS Air Force Wright Aeronautical Laboratories (MLLN) Air Force Systems Command Wright-Patterson AFB, OH 45433		10. PROGRAM ELEMENT, PROJECT, TASK AREA & WORK UNIT NUMBERS 2307P102
11. CONTROLLING OFFICE NAME AND ADDRESS Materials Laboratory (MLLN) Air Force Wright Aeronautical Laboratories Wright-Patterson Air Force Base, Ohio 45433		12. REPORT DATE December 1982 13. NUMBER OF PAGES 55
14. MONITORING AGENCY NAME & ADDRESS(if different from Controlling Office)		15. SECURITY CLASS. (of this report) UNCLASSIFIED 15a. DECLASSIFICATION DOWNGRADING SCHEDULE

16. DISTRIBUTION STATEMENT (of this Report)

Approved for public release, distribution unlimited.

17. DISTRIBUTION STATEMENT (of the abstract entered in Block 20, if different from Report)

18. SUPPLEMENTARY NOTES

J. N. Yang, Visiting Scientist, Materials Laboratory, AFWAL/MLLN, WPAFB, Ohio 45433 and Professor, School of Engineering and Applied Science, The George Washington University, Washington, D. C. 20052

19. KEY WORDS (Continue on reverse side if necessary and identify by block number)

Statistics
Statistical variability
Life Prediction
Exceedance curves
Creep crack growth
Elevated temperature
Fracture mechanics

20. ABSTRACT (Continue on reverse side if necessary and identify by block number)

A statistically-formulated fracture mechanics model for crack growth under sustained load is used to analyze crack growth data from 23 compact tension specimens of IN100, a turbojet engine disc material. The procedures characterize crack growth rates assuming that the growth rate is a lognormal random variable. The mean and standard deviation of the growth rate are determined from test data using the method of maximum likelihood. The method estimates crack growth rate parameters for each test specimen result.

DD FORM 1 JAN 73 1473 EDITION OF 1 NOV 65 IS OBSOLETE

UNCLASSIFIED

SECURITY CLASSIFICATION OF THIS PAGE (When Data Entered)

From these estimates, a lognormal creep crack growth rate model is developed from which is derived a statistical distribution of the crack size at any time. The distribution of time to reach some critical crack size is also presented. These distributions allow for the determination of the effect of hold time in the loading cycle on the life prediction of gas turbine engine discs.

PREFACE

This technical report was prepared by the Metals Behavior Branch, Metals and Ceramics Division, Materials Laboratory, Air Force Wright Aeronautical Laboratories, Wright-Patterson Air Force Base, Ohio. The research reported herein was conducted under Project No. 2307, "Solid Mechanics," Task 2307P102, "Failure Prediction in Metals." Professor J. N. Yang was engaged as a visiting scientist from the School of Engineering and Applied Science, The George Washington University, Washington, D.C. 20052.

This report covers research conducted during the period February 1982 to August 1982.

The authors are most grateful to Dr. T. Nicholas AFWAL/MLLN for his helpful suggestions, comments, and encouragement during the course of this study.

TABLE OF CONTENTS

LIST OF ILLUSTRATIONS

ILLUSTRATIONS (Continued)

LIST OF ILLUSTRATIONS (Continued)

LIST OF ILLUSTRATIONS (Concluded)

SECTION I

INTRODUCTION

Service loading spectra experienced by gas turbine engine disks include not only fatigue cyclic loadings but also sustained loads for various periods of time. Crack growth damage accumulation for engine materials occurs not only under load reversals but also under sustained loads combined with high temperatures and corrosive environments. While the crack growth behavior of engine materials due to the interactions between fatigue and sustained loads has not been understood well, analytical and experimental studies have been performed under sustained loads (e.g., References 1 and 2) or fatigue load alone (e.g., Reference 3) at high temperatures based on the fracture mechanics approach.

An experimental test program for the crack growth of IN100, a superalloy used in F100 engine disks, under sustained loads at elevated temperature has been conducted (References 1 and 2). Test results of the crack growth rate using 23 compact tension specimens obtained in References 1 and 2 indicate a considerable statistical scatter. As a result, the statistical treatment for the crack growth variability is necessary to permit a rational life prediction of gas turbine engine disks, in particular the effect of hold time in the load cycle. A fracture mechanics-based statistical model for the crack growth damage accumulation of IN100 under sustained load is proposed and investigated.

Specimen crack length records versus time were generated from load line displacement versus time data. These data were smoothed against time along with its first derivative using a seven-point averaging method making use of a least squares fit to a second-degree polynomial. By using the above, together with experimentally determined compliance versus time for each specimen, an "effective" modulus of elasticity for each specimen was determined and a smoothed effective crack length versus time record was obtained. This accounted, in part, for crack front tunneling which in IN100, when under sustained load at elevated temperature, appears to be significant. The details of data reduction are discussed in Reference 2.

The crack growth rate data alone are utilized to calibrate the fracture mechanics parameters and the statistical properties of the model using the method of maximum likelihood. A correlation study is carried out for the crack length as a function of time. From the statistical model, the distributions of the crack growth rate, the crack growth life to reach any given crack size, and the crack size at any time, have been derived. It is demonstrated that the correlation between the experimental test results and the statistical model is very reasonable.

SECTION II

TECHNICAL APPROACH

Several mathematical models were investigated for the description of the crack growth behavior of IN100 under sustained loads at elevated temperatures based on the principle of fracture mechanics (References 1 and 2). These models can be expressed in a general form

$$da(t)/dt = L(K,G,J,C^*) \tag{1}$$

in which a(t)=crack length at time t, L=a general non-negative function, K=stress intensity factor, G=strain energy release rate, J=J-integral, and C*=a line integral related to the rate of change of potential energy per unit of crack growth. A special form of L in Equation 1 was observed to be reasonable for the crack growth rate data of IN100 CT specimens,

$$\frac{da(t)}{dt} = QK^b \tag{2}$$

However, even under well-controlled laboratory conditions, crack growth rate data exhibit a considerable statistical variability. In the life prediction of engine components such a statistical scatter should be taken into account rationally; thus a statistical model based on Equation 2 is needed. We propose to randomize Equation 2 as follows;

$$\frac{da(t)}{dt} = QK^bX(K) \tag{3}$$

in which X(K) is a non-negative random function (or process) of K taking values around 1.0 to account for the random variation of the crack growth rate. Hence, the deterministic fracture mechanics model of Equation 2 represents the mean crack growth behavior whereas the statistical properties of the crack growth rate are taken care of by the random function X(K).

Two extreme cases of the random function X(K) should be mentioned. At one extreme X(K) is totally uncorrelated at any two different values of K. Based on the central limit theorem, the statistical dispersion of the crack length a(t), after integrating Equation 3, is the smallest among the class of random functions X(K) (References 4, 5). Hence, it

is unconservative for engineering analysis and design purposes. At another extreme, the random function X(K) is completely correlated at all values of K, indicating that X(K) is a random variable X. When X(K) is a random variable, a specimen with a higher (or lower) crack growth rate will maintain it throughout the entire life time. The totally correlated random function X(K)=X results in the largest statistical dispersion of the crack length a(t). Hence, it is conservative for life prediction and engineering application. It should be mentioned that instead of a random function of K, a random function of time t, i.e., X(t), can also be used (Reference 6).

When X(K) is a random function, the crack length a(t) is also a random function of time t as a consequence of Equation 3. The solution for the statistical properties of a(t) is rather involved and it may be beyond the means of current engineering discipline (Reference 6). Because of its simplicity and conservative nature for crack propagation prediction, we shall explore the extreme case in which X(K)=X is a random variable, i.e.,

$$\frac{da(t)}{dt} = QK^b X \tag{4}$$

in which X is a positive random variable taking values around unity.

Taking the logarithm of both sides of Equation 4, one obtains

$$Y = bU + q + Z \tag{5}$$

where

$$\left.\begin{aligned} Y &= \log \frac{da(t)}{dt}, \quad U = \log K \\ Z &= \log X, \quad q = \operatorname{Log} Q \end{aligned}\right\} \tag{6}$$

where Z is a random variable taking values around zero.

Now Z is assumed to be a normal random variable with zero mean and the standard deviation σ_z. Then it follows from Equation 5 that the log crack growth rate Y = log da(t)/dt is also a normal random variable with the mean value μ_y and standard deviation σ_y given by

$$\mu_y = bU + q \tag{7}$$

$$\sigma_y = \sigma_z \tag{8}$$

The parameters b and q (or Q) as well as the standard deviation σ_z (or σ_y) can be estimated from the test results of the crack growth rate versus stress intensity factor using Equation 5 and the method of maximum likelihood. Since Y and Z are normal random variables and Equation 5 is linear, the method of maximum likelihood is identical to the linear regression analysis and the method of least squares.

Test results of the crack growth rate versus stress intensity factor for IN100 CT specimens at 1350°F have been generated for five different thicknesses. The results are presented in Figures 1(a) through 1(e). The method of maximum likelihood has been used to estimate the values of b, Q, and $\sigma_y = \sigma_z$ for five test groups and the results are shown in Table 1 on page 9. The straight lines in Figures 1(a) through 1(e) represent the estimated mean values $\mu_y = bU + q$ (Equation 7).

Each datum in Figures 1(a) through 1(e) is calculated from a one-to-one corresponding crack growth-versus-time and specimen load line displacement-versus-time measurement using a seven-point averaging method to smooth the time records. Crack lengths were computed from experimental compliance based on an exact solution for load line displacements (Reference 2).

The initial crack growth rates for the 23 specimens were observed to start from an initially high rate and then decrease to a level which corresponded to the onset of stable creep crack growth. This decrease in the initial crack growth rates was due to an initially decreasing load line displacement rate, upon which the calculations of crack lengths rested. These initially decreasing rates were excluded from the analysis performed herein.

To show the validity of the assumption that Z follows the normal distribution, sample values of Z denoted by z_j, are computed from the test results of the log crack growth rate Y = log da(t)/dt versus the

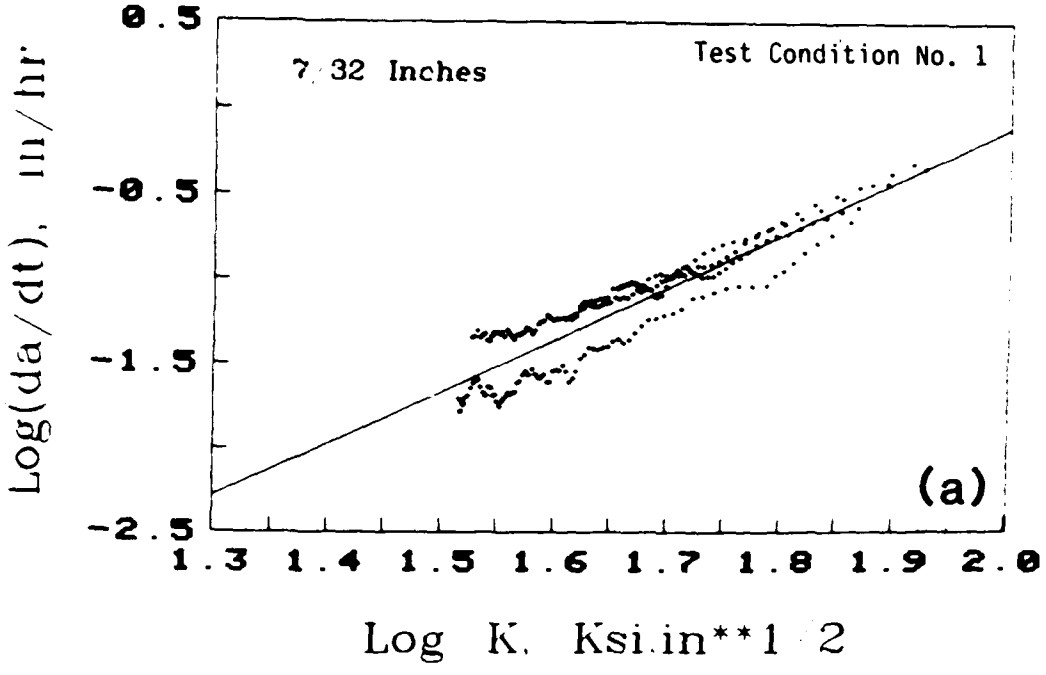

Figure 1(a). Log Crack Growth Rate Versus Log Stress Intensity Factor for Various Thickness Specimen Group; 7/32 Inches.

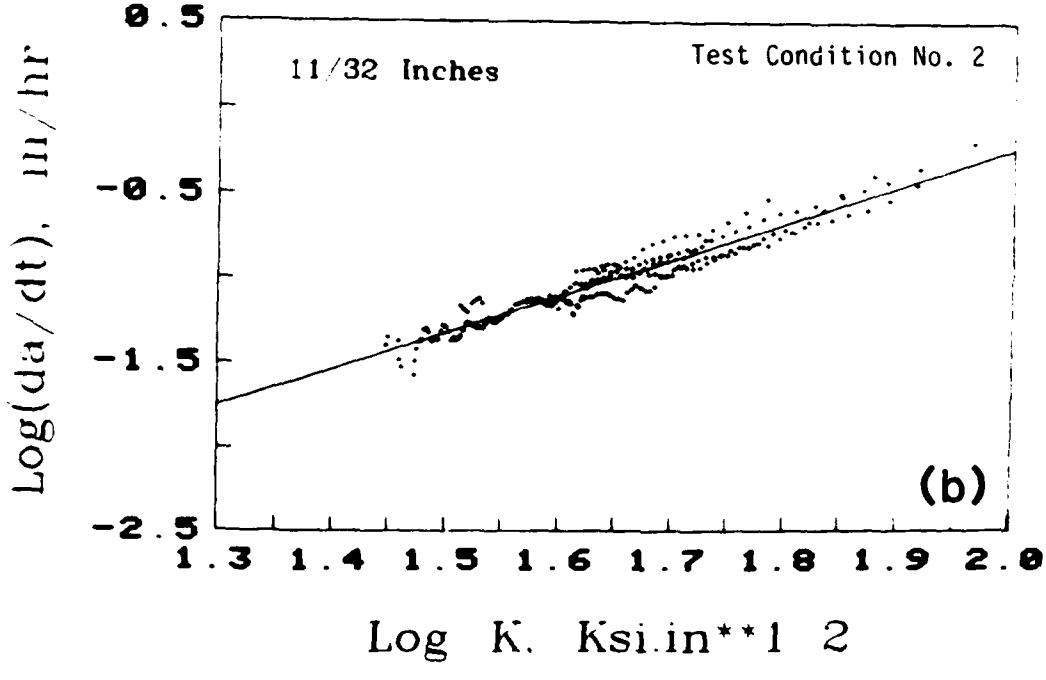

Figure 1(b). Log Crack Growth Rate Versus Log Stress Intensity Factor for Various Thickness Specimen Group; 11/32 Inches.

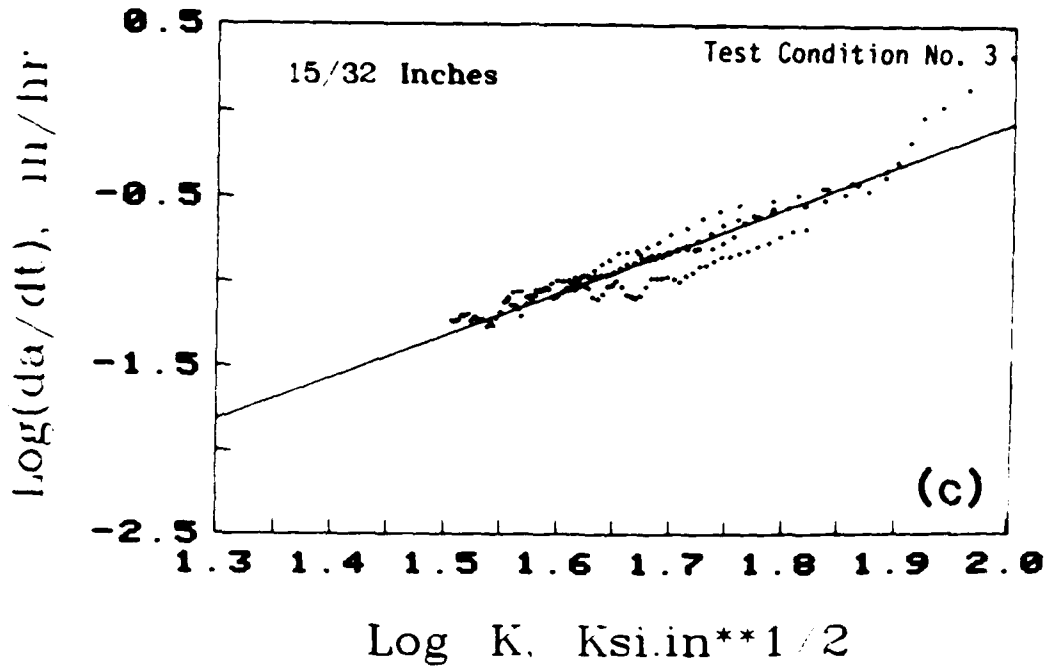

Figure 1(c). Log Crack Growth Rate Versus Log Stress Intensity Factor for Various Thickness Specimen Group; 15/32 Inches.

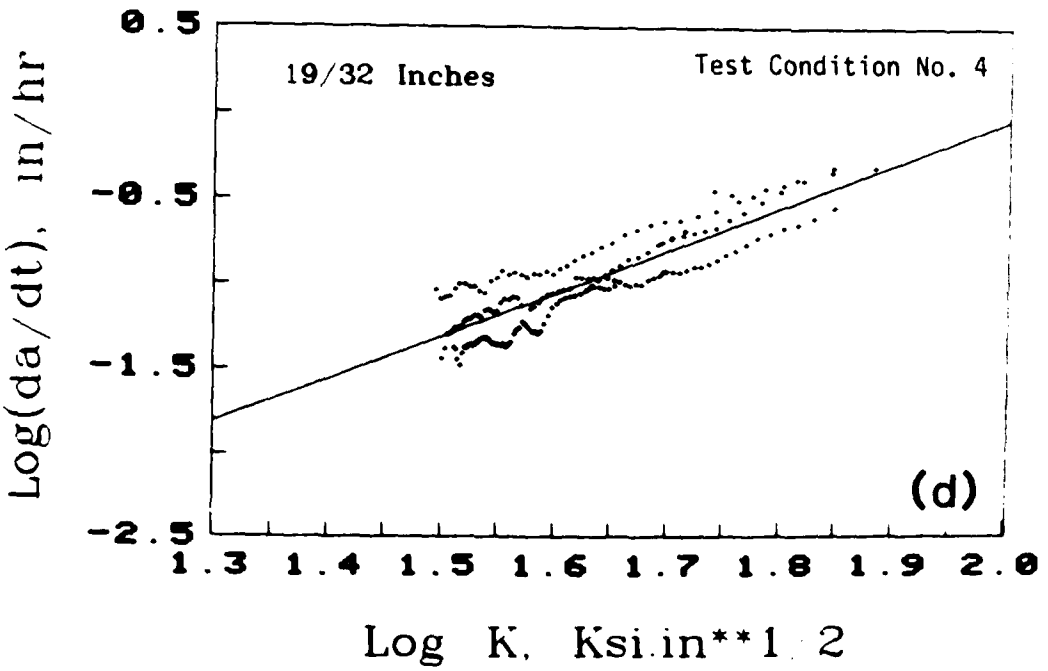

Figure 1(d). Log Crack Growth Rate Versus Log Stress Intensity Factor for Various Thickness Specimen Group; 19/32 Inches.

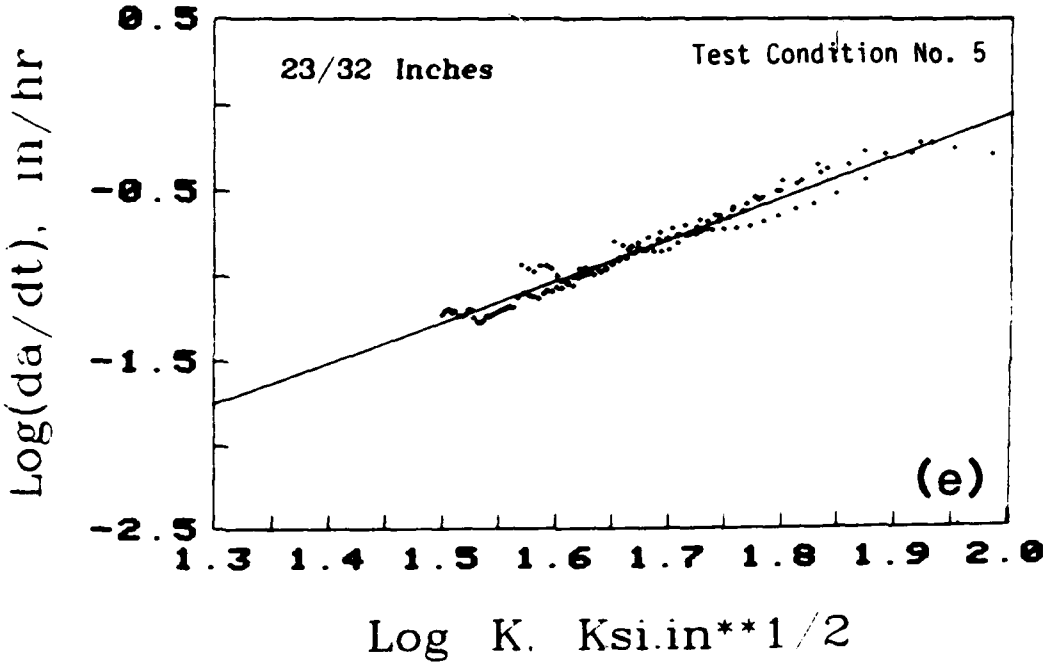

Figure 1(e). Log Crack Growth Rate Versus Log Stress Intensity Factor for Various Thickness Specimen Group; 23/32 Inches.

log stress intensity factor U = log K, denoted by (y_j, u_j), using Equation 5

$$z_j = y_j - bu_j - q \quad \text{for } j=1,2,\ldots,n \tag{9}$$

in which b and q have been estimated by the method of maximum likelihood and n is the total number of test data.

Sample data of z_j (j=1,2,...,n) obtained from Figure 1(b) are plotted on normal probability paper in Figure 2 as circles along with a straight line representing the estimated normal distribution of Z (with zero mean and standard deviation σ_z determined previously, see Table 1). A linear scale is used in Figure 2 in which the sample data z_j are arranged in ascending order, i.e., $z_1 \leq z_2 \leq z_3 \ldots \leq z_n$, and the ordinate corresponding to z_j is given by $\Phi^{-1}[j/(n+1)]$ with $\Phi^{-1}(\ )$ being the inversed standardized normal distribution function. It is observed from Figure 2 that the sample values of Z are scattered around the straight line without a nonlinear trend, indicating that the normal distribution is acceptable.

TABLE 1

MAXIMUM LIKELIHOOD ESTIMATE OF b, Q, STANDARD DEVIATION σ_y AND COEFFICIENT OF VARIATION OF da/dt

Thickness (Inch)	b	Q	$\sigma_y = \sigma_z$	Coef. of Variation	No. of Points	No. of Specimens
7/32	3.1015	4.8563×10^{-7}	0.13325	31.42%	233	4
11/32	2.1626	2.7349×10^{-5}	0.06796	15.75%	227	5
15/32	2.4995	8.6942×10^{-6}	0.09550	22.30%	156	4
19/32	2.5255	8.0931×10^{-6}	0.12870	30.30%	185	5
23/32	2.4220	1.2594×10^{-5}	0.05740	13.28%	132	4

The Kolmogorov-Smirnov test for goodness of fit has been performed to determine the observed K-S statistic D_n. It is shown that the normal distribution is acceptable at least at a 10% level of significance.

Since Z=log X and Y=log da(t)/dt are normal random variables, the crack growth rate G=da(t)/dt follows the lognormal distribution. The

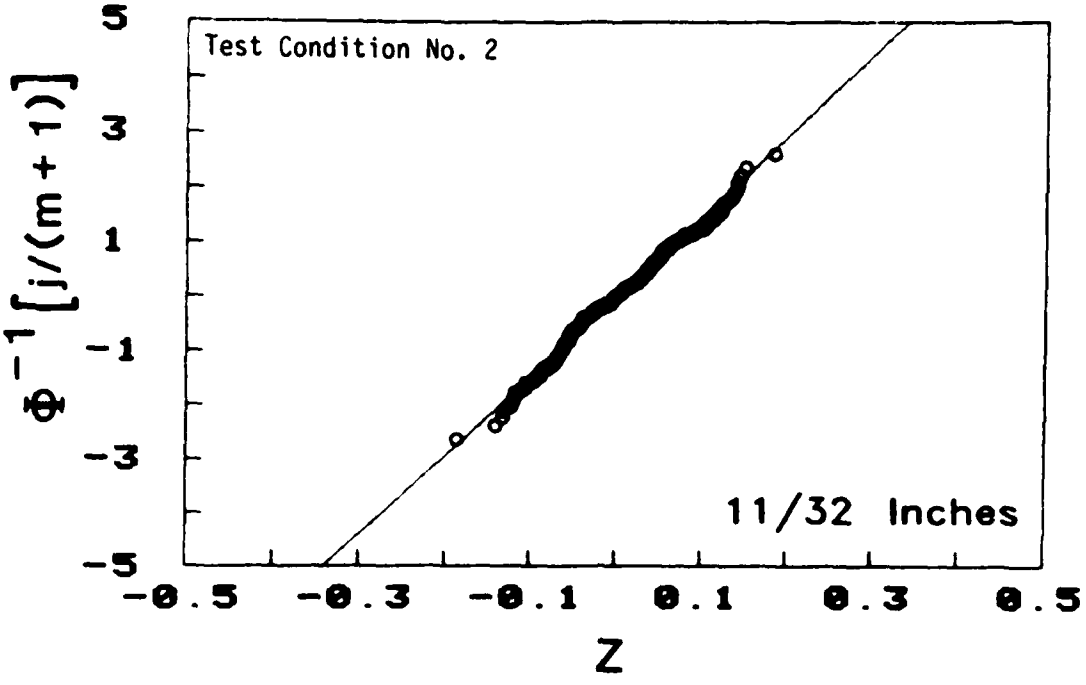

Figure 2. Normal Probability Plot for Z for 11/32 Inches Thick Specimen Group.

coefficient of variation, V, of da(t)/dt is related to the standard deviation $\sigma_y=\sigma_z$ through

$$V = \left[e^{(\sigma_y \ln 10)^2} - 1 \right]^{1/2} \tag{10}$$

Test results of the coefficient of variation V for the crack growth rate G=da(t)/dt for five test groups are presented in Table 1.

It is interesting to mention that the coefficient of variation, V, which is a measure of the statistical dispersion of the crack growth rate for IN100 CT specimens under fatigue cyclic loadings at elevated temperatures reported in Reference 4, is larger than that of the same specimen under sustained loads obtained in this report.

The distribution of Z and Y=log[da(t)/dt] are both normal with the same standard deviation $\sigma_z=\sigma_y$ that has been determined previously. Let z_γ be the γ precentile of Z, i.e.,

$$\gamma\% = P[Z>z_\gamma] = 1 - \Phi(z_\gamma/\sigma_z) \tag{11}$$

or inversely,

$$z_\gamma = \sigma_z \, \Phi^{-1}(1 - \gamma\%) \tag{12}$$

The γ percentile of the log crack growth rate Y, denoted by y_γ follows from Equation 5 as

$$y_\gamma = bU + q + z_\gamma \tag{13}$$

in which z_γ is given by Equation 12.

Therefore, by varying the value of γ, one obtains the distribution of the log crack growth rate in terms of percentiles. The results are shown in Figure 3 for the second test group. As an example, the crack growth rate path associated with γ=10 indicates that 10% of specimens will have a growth rate faster than that shown by the curve.

The γ percentile of the random variable X, denoted by X_γ, is computed from Equation 6 as

$$X_\gamma = (10)^{z_\gamma} \tag{15}$$

in which z_γ is given by Equation 12.

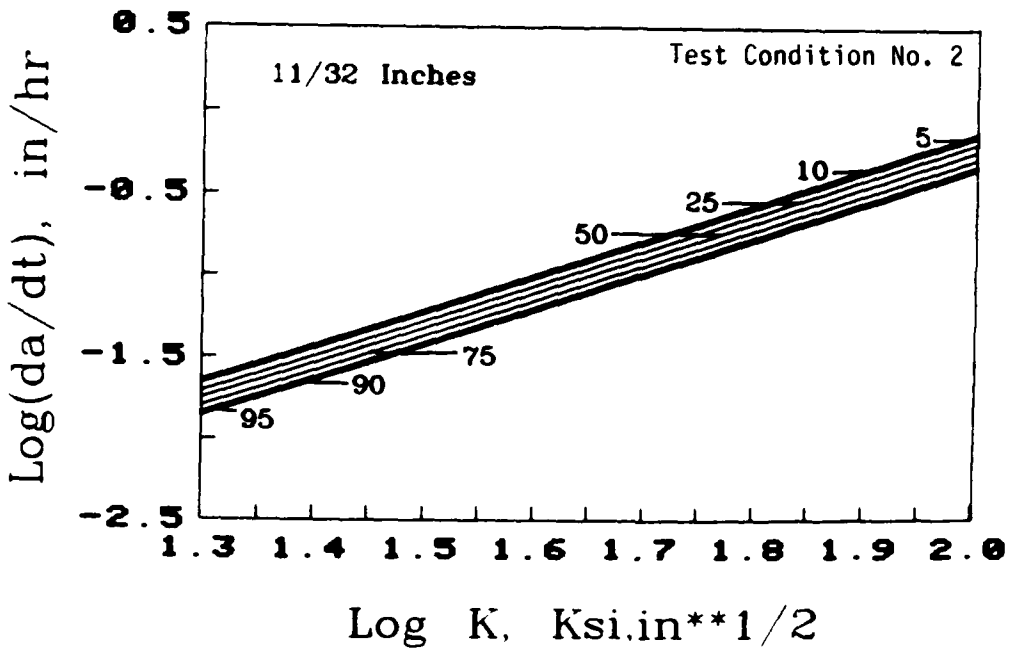

Figure 3. Percentiles of Log Crack Growth Rate Y as a Function of Log Stress Intensity Factor X for 11/32 Inches Thick Specimen Group (Theoretical Model).

The γ percentile of the crack length a(t) at time t, denoted by $a_\gamma(t)$, is obtained by substituting Equation 15 into Equation 4

$$\frac{da_\gamma(t)}{dt} = QK^b X_\gamma \tag{16}$$

in which the stress intensity factor K of the compact tension specimen is expressed as

$$K = \frac{P}{B\sqrt{W}} f[a_\gamma(t)] \tag{17}$$

where B=thickness of the specimen, W=width of the specimen, P=applied load and

$$f[a_\gamma(t)] = \frac{2+\alpha}{(1-\alpha)^{3/2}} (0.866 + 4.64\alpha - 13.32\alpha^2 + 14.72\alpha^3 - 5.6\alpha^4) \tag{18}$$

$$\alpha = \frac{a_\gamma(t)}{W} \tag{19}$$

Thus, Equation 16 can be integrated numerically over particular limits to obtain a set of crack length $a_\gamma(t)$ versus time t for different γ percentiles as shown in Figure 4. The integrations were performed for an ASTM compact tension specimen with thickness B = 11/32 inch (8.73 mm), width W = 2.5 inches (63.5 mm), maximum load P = 3.17 kips (14.1kN), initial crack length a(0) = 0.68 inch (17.3 mm) and final crack length a(t) = 1.25 inch (31.75 mm). It should be mentioned that the numerical integration of Equation 16 for each γ percentile of the crack length, $a_\gamma(t)$, is deterministic and straightforward.

In the life prediction of engine components, two statistical distributions are of practical importance; (1) the distribution function, $F_{T(a)}(t)$, of the time, T(a), to reach any given crack length, a, and (2) the distribution function, $F_{a(t)}(u)$, of the crack length, a(t), at any time t. It has been shown in Reference 4 that both distributions are related and one can be derived from the other.

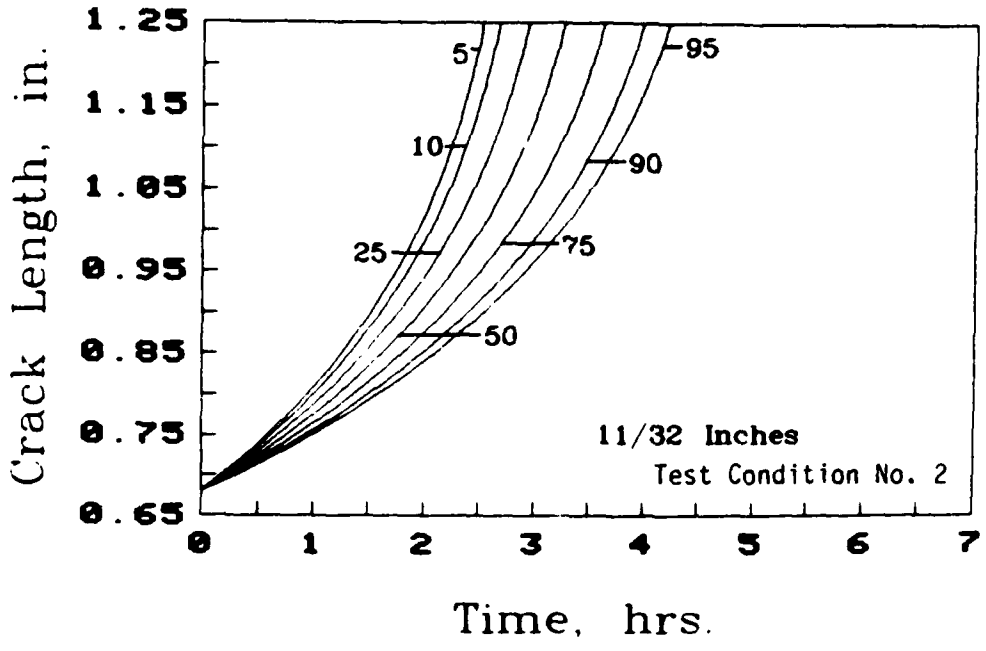

Figure 4. Percentiles of Crack Length a(t) as Function of Time t (Theoretical Model) for 11/32 Inches Thick Specimen Group.

Since Figure 4 represents the distribution of the crack length as a function of time t, it contains all the information needed to determine the distributions mentioned previously. For instance, by drawing a horizontal line in Figure 4 through a crack length of interest, the distribution of time to reach that crack length is obtained. Likewise, drawing a vertical line in Figure 4 through a given time t, one obtains the distribution of the crack length at that time instant. The complement $F^*_{a(t)}(u)$ of the distribution function $F_{a(t)}(u)$ of the crack length, i.e., $F^*_{a(t)}(u)=1=F_{a(t)}(u)$, is the probability that the crack length at time t will exceed certain length u. Hence, $F^*_{a(t)}(u)$ is referred to as the crack exceedance curve.

The distribution function $F_{T(a)}(t)$ for the time to reach the crack lengths a=0.75, 0.85, 0.95, and 1.25 inches (19.05, 21.6, 24.1 and 31.75 mm, respectively) are obtained from Figure 4 and displayed in Figure 5 as solid curves. The crack exceedance curve $F^*_{a(t)}(u)$ at t=2.5 hours is shown in Figure 6 as a solid curve.

It should be emphasized that the numerical integration of Equation 16 for each γ percentile of the crack length, $a_\gamma(t)$, is deterministic and straightforward. As a result, it is very easy to construct the distribution of the crack length as a function of time given by Figure 4. Thus, the present statistical model is very simple for practical applications.

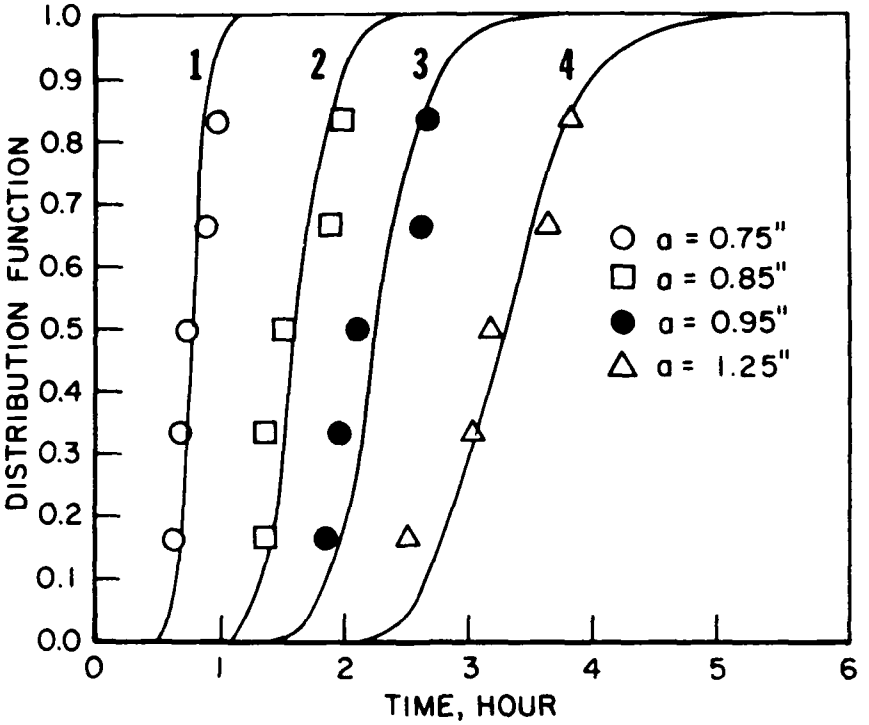

Figure 5. Distribution of Time to Reach Given Crack Lengths a = 0.75, 0.85, 0.95, and 1.25 Inches for 11/32 Inches Thick Specimen Group (Solid Curves are Theoretical Model).

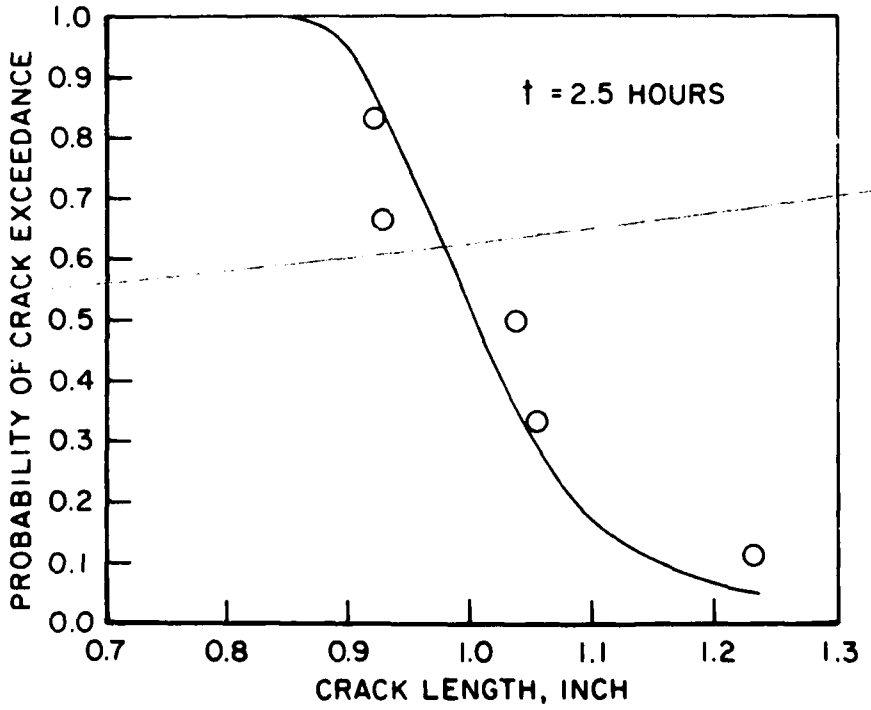

Figure 6. Probability of Crack Exceedance at 2.5 Hours for 11/32 Inches Thick Specimen Group (Solid Curve is Theoretical Model).

SECTION III

CORRELATION WITH TEST RESULTS

A problem in the correlation study is that the number of specimens in each thickness group is very small (Table 1) and even with such a small sample size each specimen is usually tested using different initial flaw length, a(0), final flaw length, a_F, and applied load P. The loading conditions for each specimen were given in Reference 2. Thus the test results of the crack length a(t) are not homogeneous.

Fortunately, the present statistical model utilizes only the crack growth rate versus the stress intensity data (Figure 1) to calibrate all the fracture mechanics parameters without using the test results of the crack length a(t) versus time t. To study the correlation between the statistical model, and the test results, in terms of the crack growth damage accumulation, a(t), versus time, t, including the distribution of time to reach any given crack length, and the distribution of the crack length at any time instant t, homogeneous test conditions were assumed for each thickness group as shown in Table 2. The applied loads P used in Table 2 were chosen to avoid excessive extrapolation into the region of the stress intensity factor K where no actual data existed (Figures 1(a)-1(e)).

TABLE 2

ASSUMED HOMOGENEOUS TEST ENVIRONMENTS FOR STANDARD COMPACT TENSION TEST SPECIMENS

Thickness (in.)	a(0) (in.)	a_F (in.)	P (kips)
7/32	0.66	1.25	2.28
11/32	0.68	1.25	3.17
15/32	0.68	1.25	4.39
19/32	0.68	1.25	4.08
23/32	0.68	1.25	5.89

Note: a(0) = Initial Flaw Length, a_F = Final Flaw Length,
P = Applied Load

Test results of the crack growth rate for each specimen are best fitted by Equation 2 using the method of least squares to estimate the values of b and Q. Sample values of b and Q for each specimen are presented in Table 3 for various thickness group. The best fitted crack growth rate is shown in Figure 7 as a straight line for the first specimen in each thickness group, along with the test data. It should be mentioned that the crack growth curves, a(t) versus time t, obtained by integrating the test data of Figure 7, are indistinguishable from those determined by integrating the best fitted straight line. In other words, the resulting crack length a(t) versus time t obtained by integrating Equation 2 and using the values of b and Q given in Table 3 are essentially identical to that obtained by integrating the actual crack growth rate data. This justifies the correlation study of the crack length using the assumed homogeneous test conditions given in Table 2.

TABLE 3

BEST FITTED b AND Q VALUES FOR EACH SPECIMEN IN ALL THICKNESS GROUPS

Specimen No.	b	Q	Specimen No.	b	Q
7/32 Inches Thickness Group			15/32 Inches Thickness Group		
1	2.6559	3.4359×10^{-6}	1	2.9257	1.8229×10^{-6}
2	3.0959	3.4359×10^{-7}	2	2.5697	7.6367×10^{-6}
3	2.8626	1.4920×10^{-6}	3	1.8834	7.2033×10^{-5}
4	2.4962	5.7090×10^{-6}	4	2.2316	2.4520×10^{-5}
11/32 Inches Thickness Group			19/32 Inches Thickness Group		
1	2.1847	2.1388×10^{-5}	1	3.7926	6.3718×10^{-8}
2	1.4166	5.5907×10^{-4}	2	2.4683	1.0241×10^{-5}
3	2.1912	2.6118×10^{-5}	3	2.1385	5.1545×10^{-5}
4	2.7300	3.7005×10^{-6}	4	2.1953	2.2517×10^{-5}
5	2.6969	2.9139×10^{-6}	5	2.9969	1.4040×10^{-6}
23/32 Inches Thickness Group					
1	1.9285	8.3606×10^{-5}			
2	2.7192	4.1785×10^{-6}			
3	2.6142	5.9990×10^{-6}			
4	2.6729	4.8845×10^{-6}			

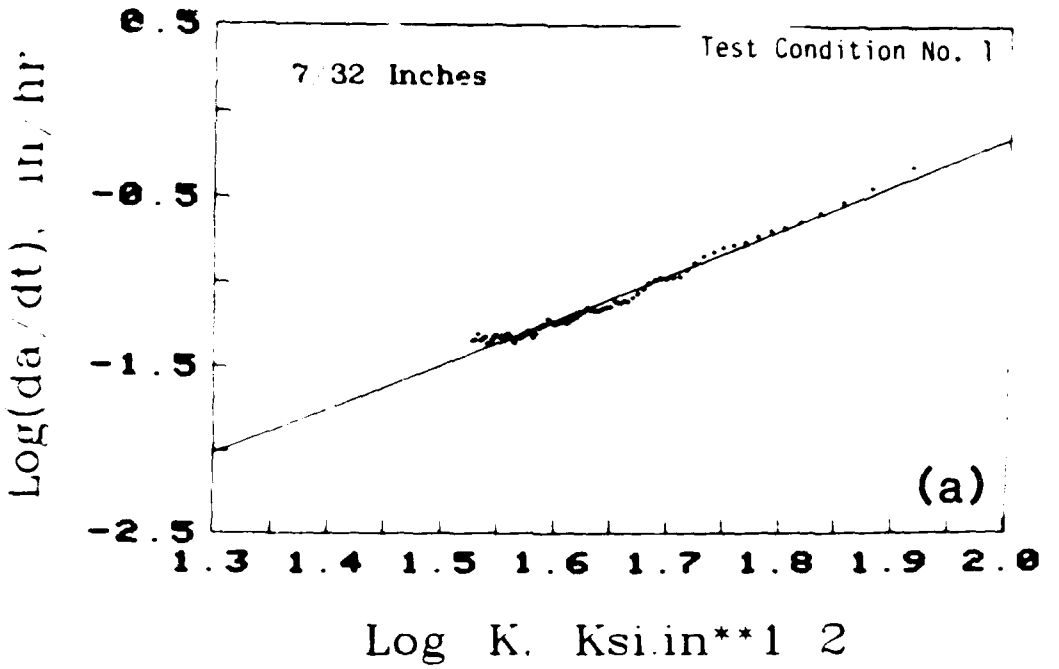

Figure 7(a). Best Fitted Crack Growth Rate Data for the First Specimen in Each Thickness Group; 7/32 Inches.

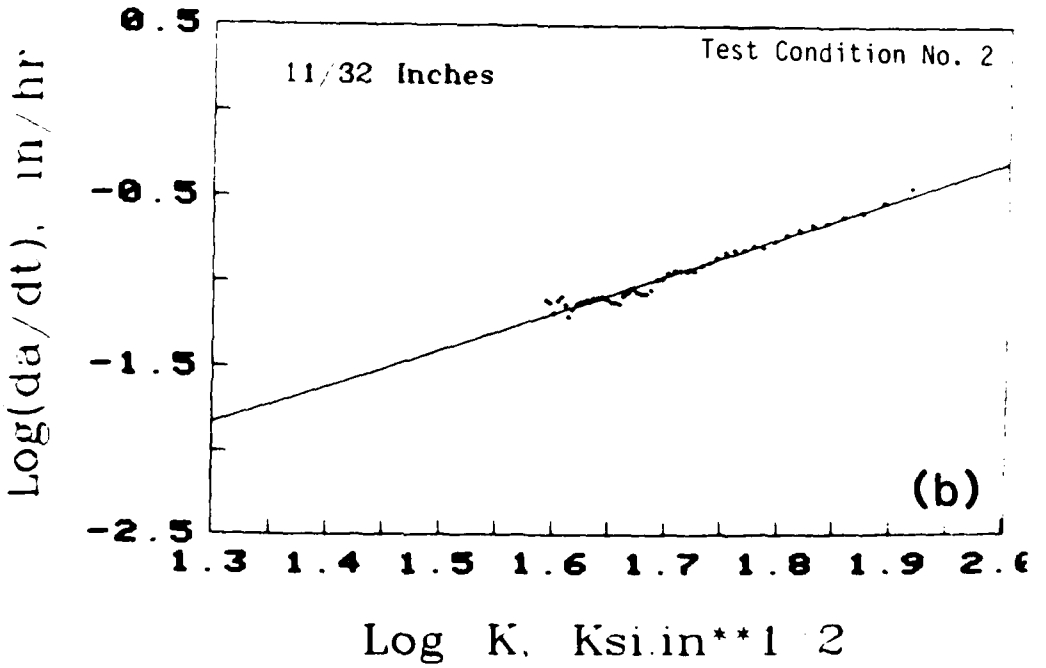

Figure 7(b). Best Fitted Crack Growth Rate Data for the First Specimen in Each Thickness Group; 11/32 Inches.

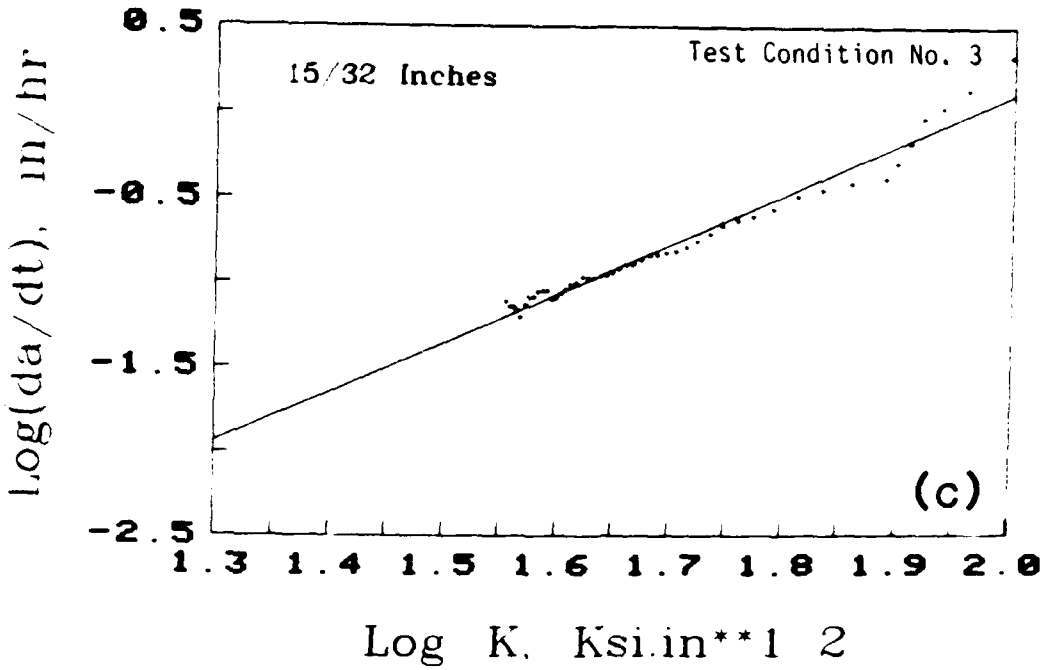

Figure 7(c). Best Fitted Crack Growth Rate Data for the First Specimen in Each Thickness Group; 15/32 Inches.

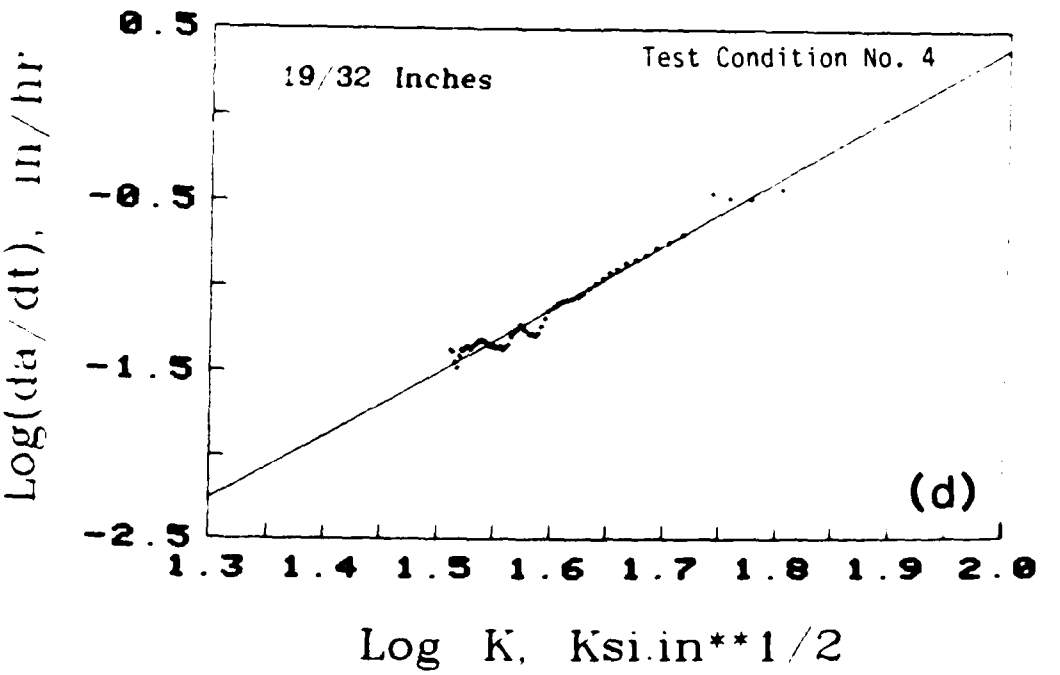

Figure 7(d). Best Fitted Crack Growth Rate Data for the First Specimen in Each Thickness Group; 19/32 Inches.

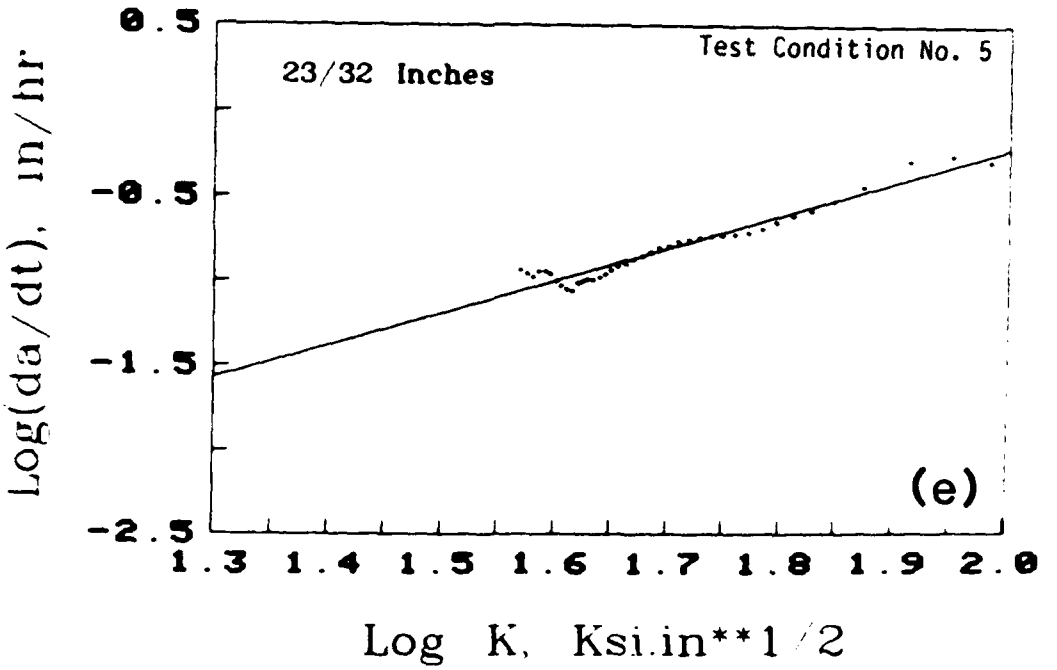

Figure 7(e). Best Fitted Crack Growth Rate Data for the First Specimen in Each Thickness Groupl 23/32 Inches.

On the basis of the statistical model, the maximum likelihood estimate of b, Q and σ_y obtained in Table 1 are used to construct various percentiles of the log crack growth rate Y=log da/dt versus log stress intensity factor U=log K. The results for five thickness groups are shown in Figures 8(a)-12(a) for γ = 5, 10, 25, 50, 75, 90 and 95 percentiles. The least square estimates of b and Q for each individual specimen given in Table 3 are used in conjunction with Equation 2 to construct Y versus U, and the results are displayed in Figures 8(b)-12(b). Figures 8(b)-12(b) are referred to as the extrapolated test results, since the actual test data do not exist in the entire range of K.

The crack growth rates shown in Figures 8-12 have been integrated over the limits given in Table 2, the assumed homogeneous test conditions, to yield crack length, a(t), versus time, t. The corresponding results are depicted in Figures 13-17 for five thickness groups (again curves in Figures 13(a)-17(a) represent γ = 5, 10, 25, 50, 75, 90 and 95 percentiles). A comparison between Figures 13(a)-17(a) and Figures 13(b)-17(b) indicates that the correlation between the statistical model and the extrapolated test results is very reasonable.

Based on the statistical model, the distribution function, $F_{T(a)}(t)$, for the time T(a) to reach crack lengths 0.75, 0.85, 0.95, and 1.25 inches (19.05, 21.6, 24.1 and 31.75 mm, respectively) are obtained by drawing horizontal lines through appropriate crack lengths in Figures 13(a)-17(a) and the results are plotted in Figures 18-22 as solid curves designated, respectively, by Curves 1, 2, 3 and 4. The corresponding distribution functions for the extrapolated test results are obtained from Figures 13(b)-17(b) and displayed in Figures 18-22 as circles, squares, solid circles and triangles, respectively. In constructing the distribution function for the extrapolated test results shown in Figure 18 for instance, a horizontal line is drawn through the given crack length in Figure 13(b) to obtain four data points. These four data points are ranked in an ascending order and the ordinate of the ith data point is i/(m+1) where m=4 is the total number of points. Figures 18-22 demonstrate a good correlation between the statistical model (solid curves indicated by 1, 2, 3 and 4) and the extrapolated test results (circles, squares, solid circles and traingles).

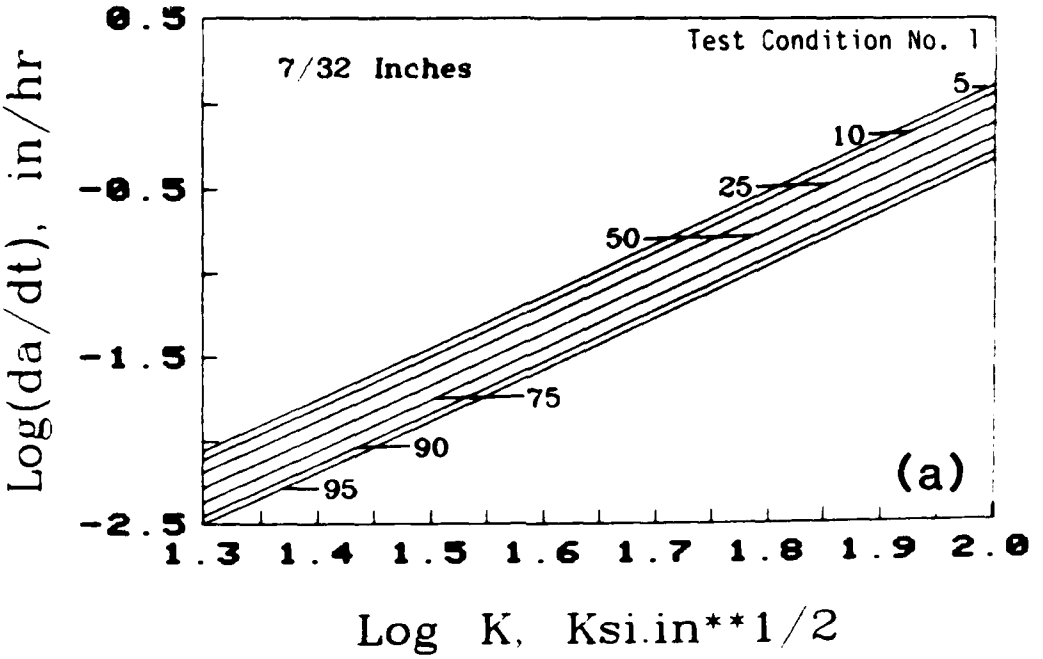

Figure 8(a). Log Crack Growth Rate Y Versus Log Stress Intensity Factor for 7/32 Inches Thickness Group; Statistical Model.

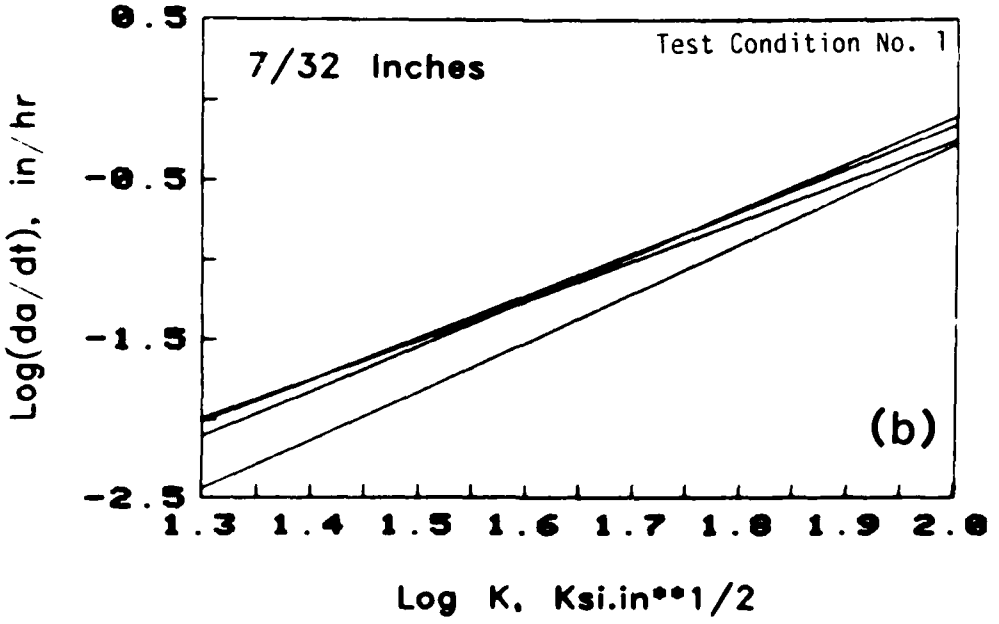

Figure 8(b). Log Crack Growth Rate Y Versus Log Stress Intensity Factor for 7/32 Inches Thickness Group; Extrapolated Test Results.

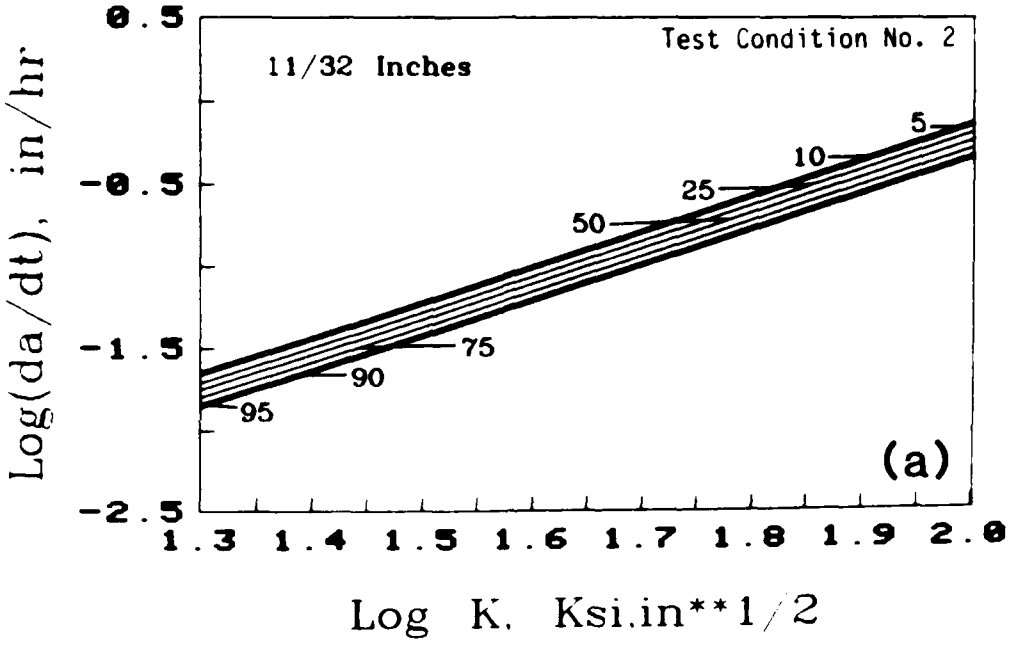

Figure 9(a). Log Crack Growth Rate Y Versus Log Stress Intensity Factor for 11/32 Inches Thickness Group; Statistical Model.

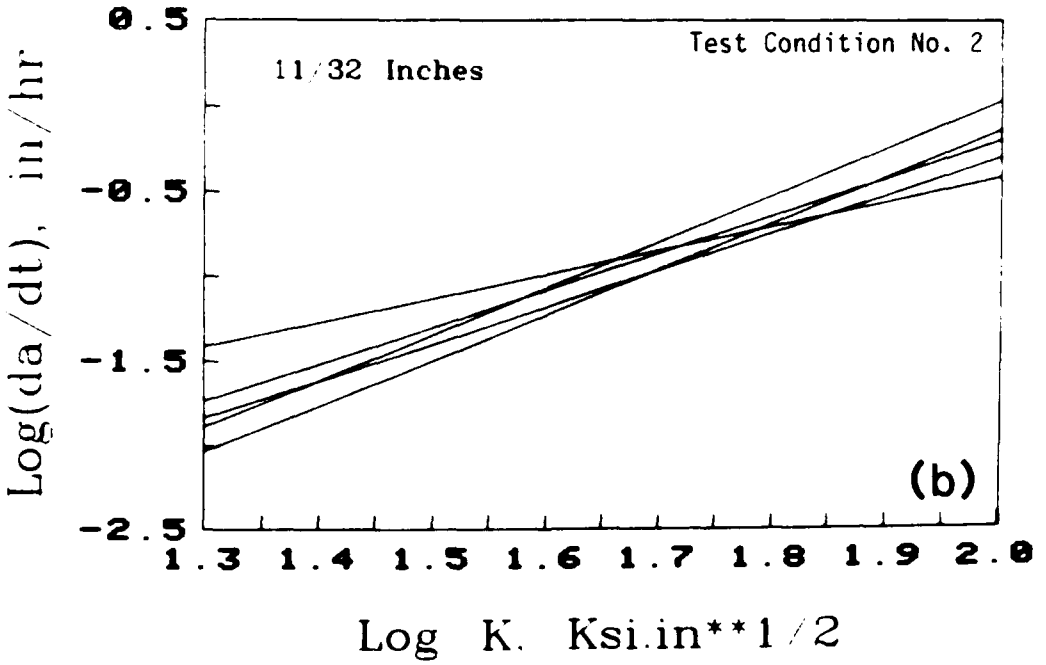

Figure 9(b). Log Crack Growth Rate Y Versus Log Stress Intensity Factor for 11/32 Inches Thickness Group; Extrapolated Test Results.

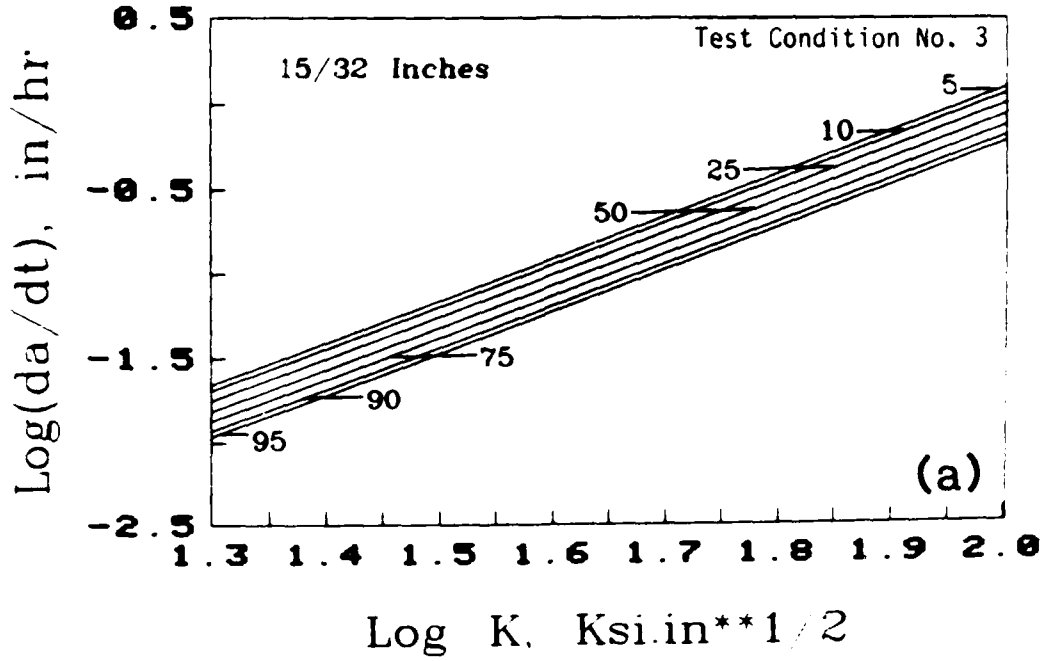

Figure 10(a). Log Crack Growth Rate Y Versus Log Stress Intensity Factor for 15/32 Inches Thickness Group; Statistical Model.

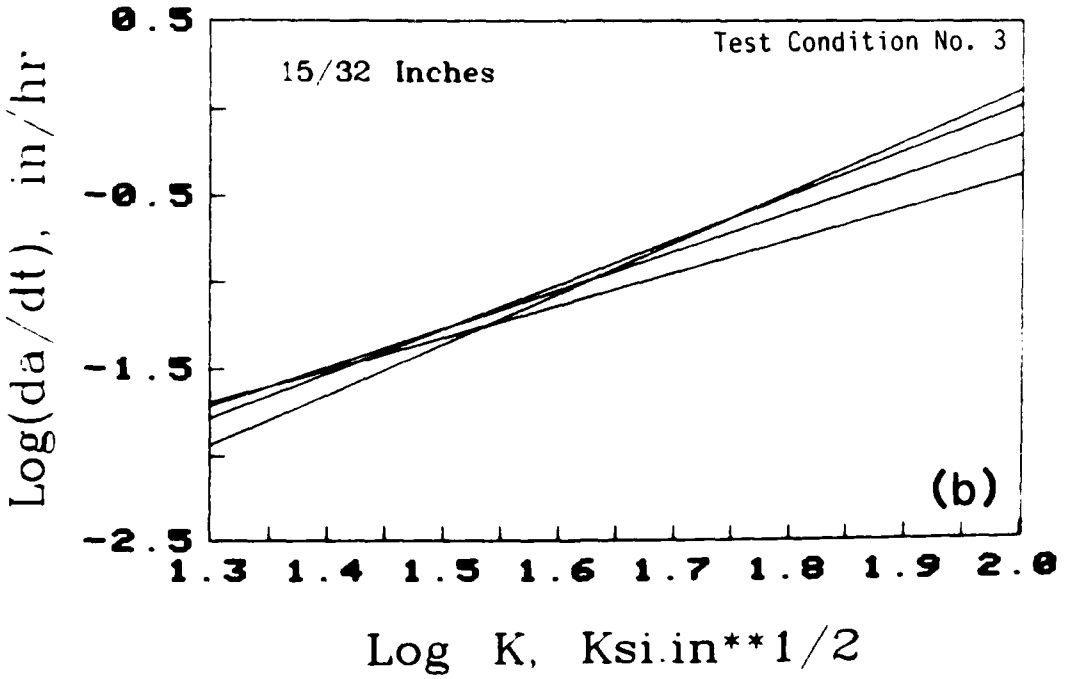

Figure 10(b). Log Crack Growth Rate Y Versus Log Stress Intensity Factor for 15/32 Inches Thickness Group; Extrapolated Test Results.

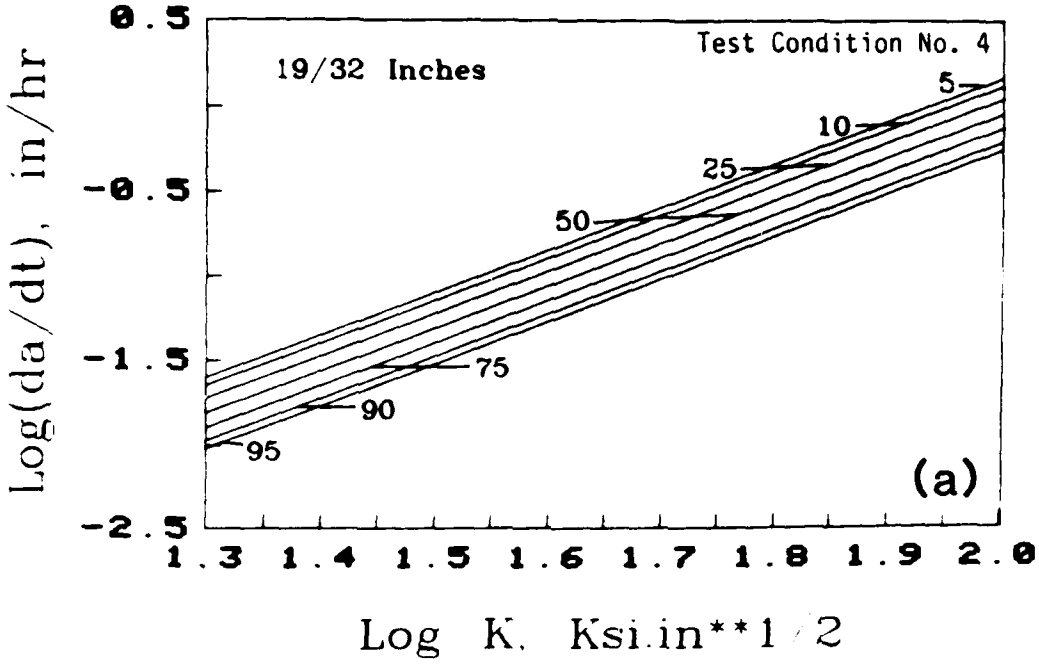

Figure 11(a). Log Crack Growth Rate Y Versus Log Stress Intensity Factor for 19/32 Inches Thickness Group; Statistical Model.

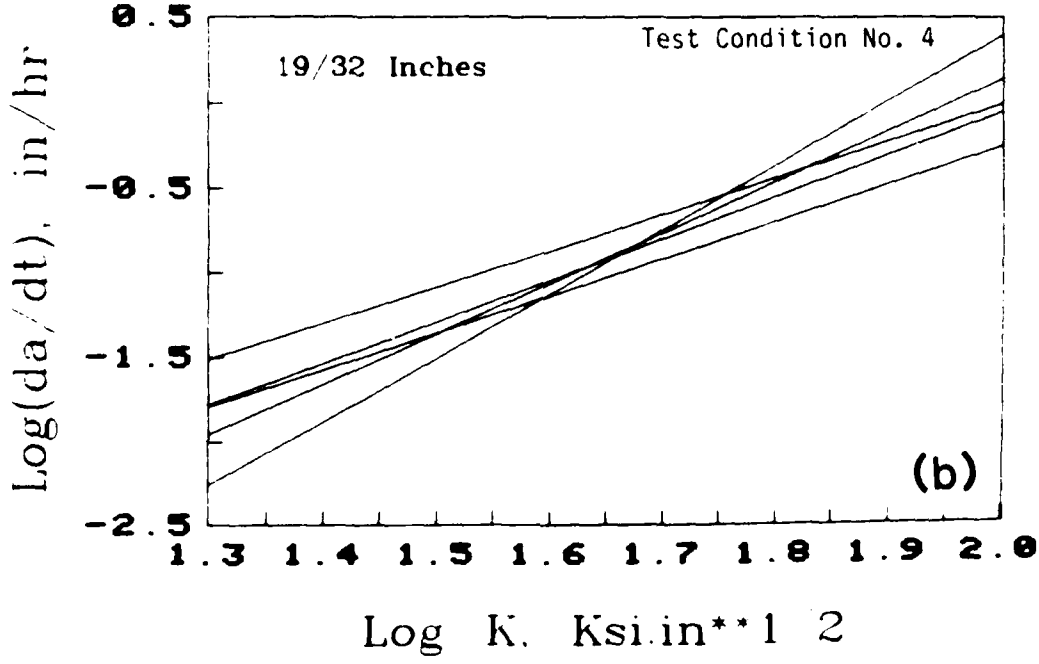

Figure 11(b). Log Crack Growth Rate Y Versus Log Stress Intensity Factor for 19/32 Inches Thickness Group; Extrapolated Test Results.

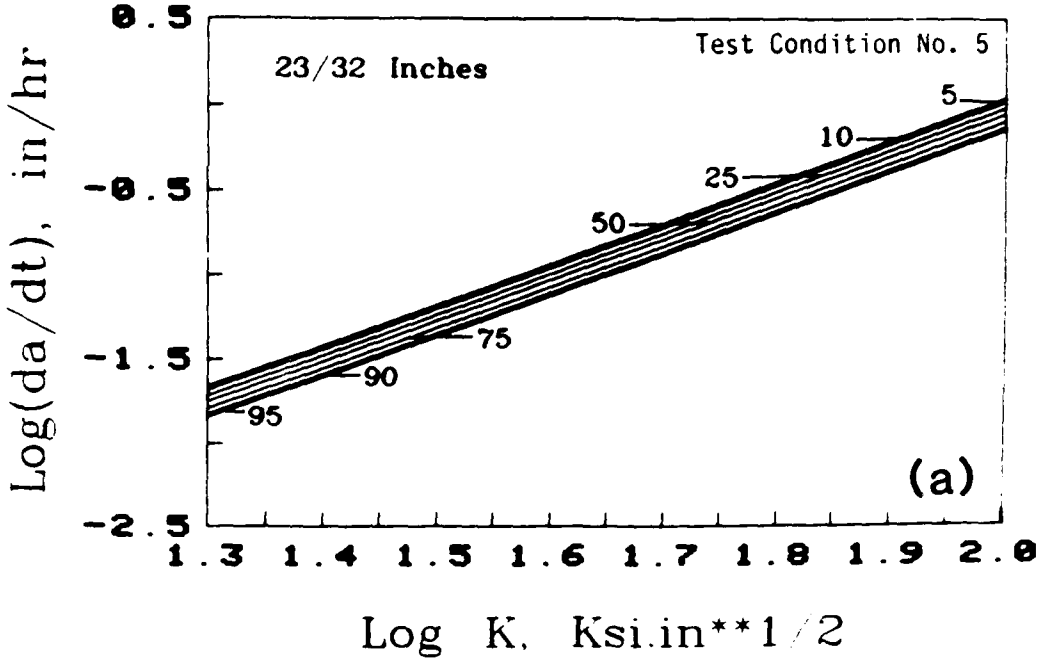

Figure 12(a). Log Crack Growth Rate Y Versus Log Stress Intensity Factor for 23/32 Inches Thickness Group; Statistical Model.

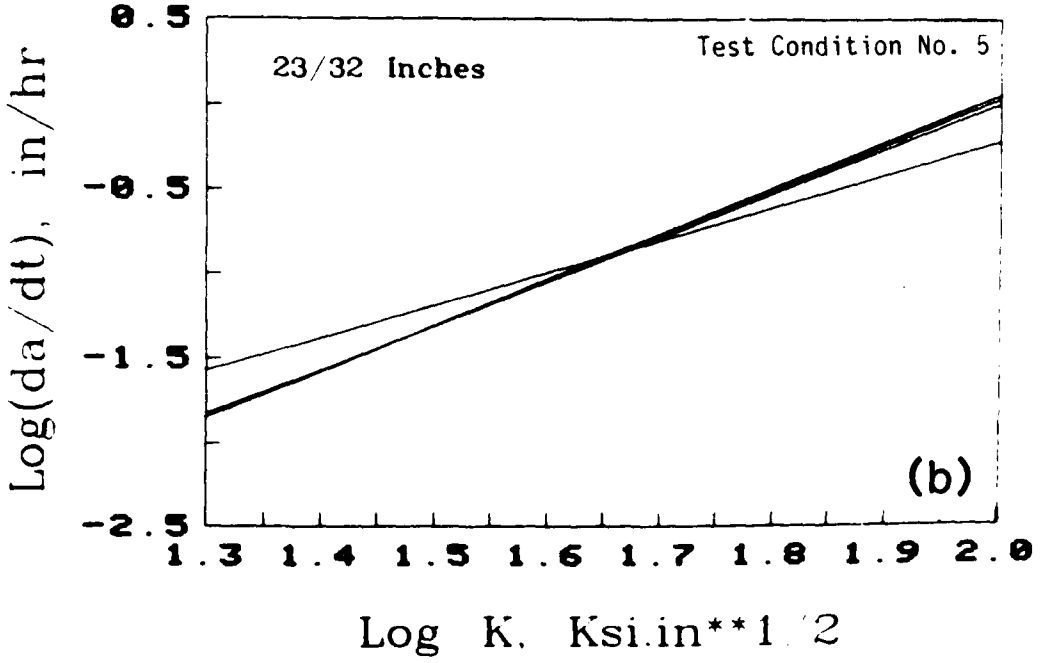

Figure 12(b). Log Crack Growth Rate Y Versus Log Stress Intensity Factor for 23/32 Inches Thickness Group; Extrapolated Test Results.

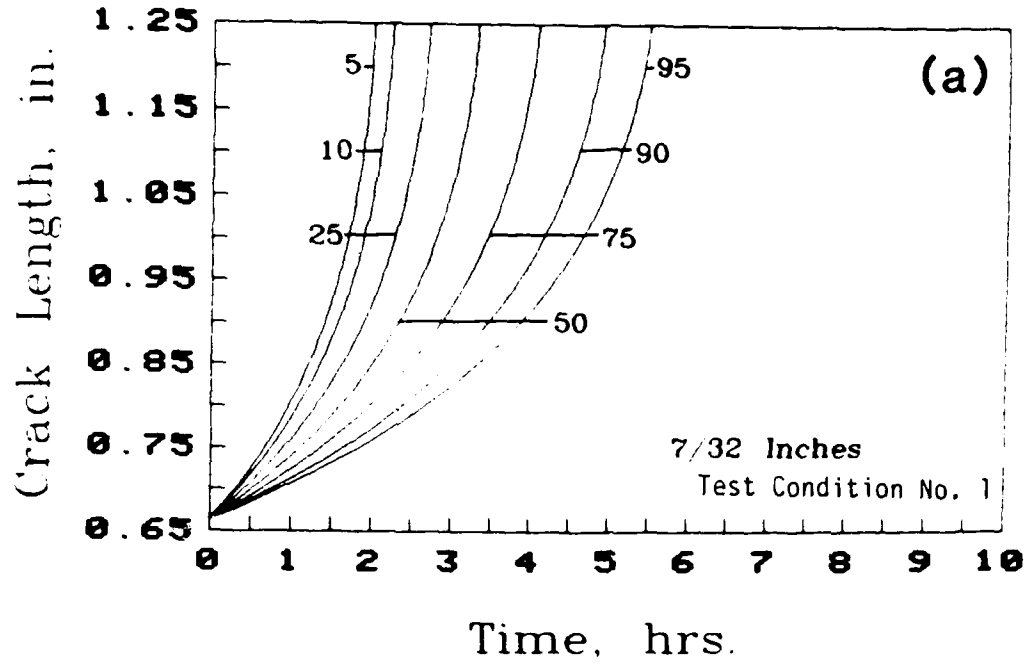

Figure 13(a). Crack Length a(t) Versus Time t for 7/32 Inches Thickness Group; Statistical Model.

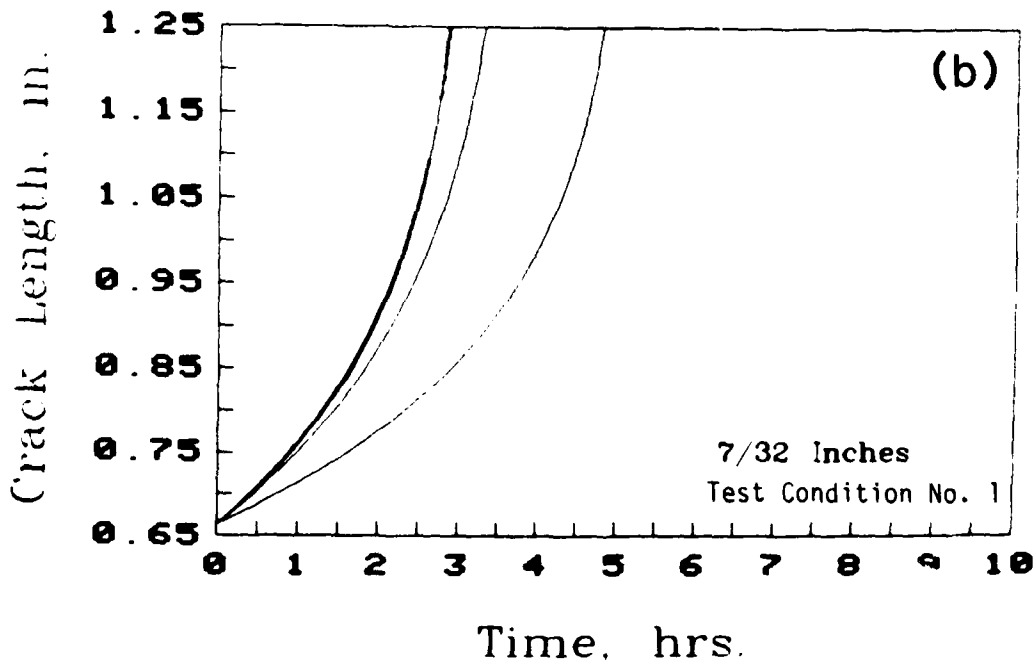

Figure 13(b). Crack Length a(t) Versus Time t for 7/32 Inches Thickness Group; Extrapolated Test Results.

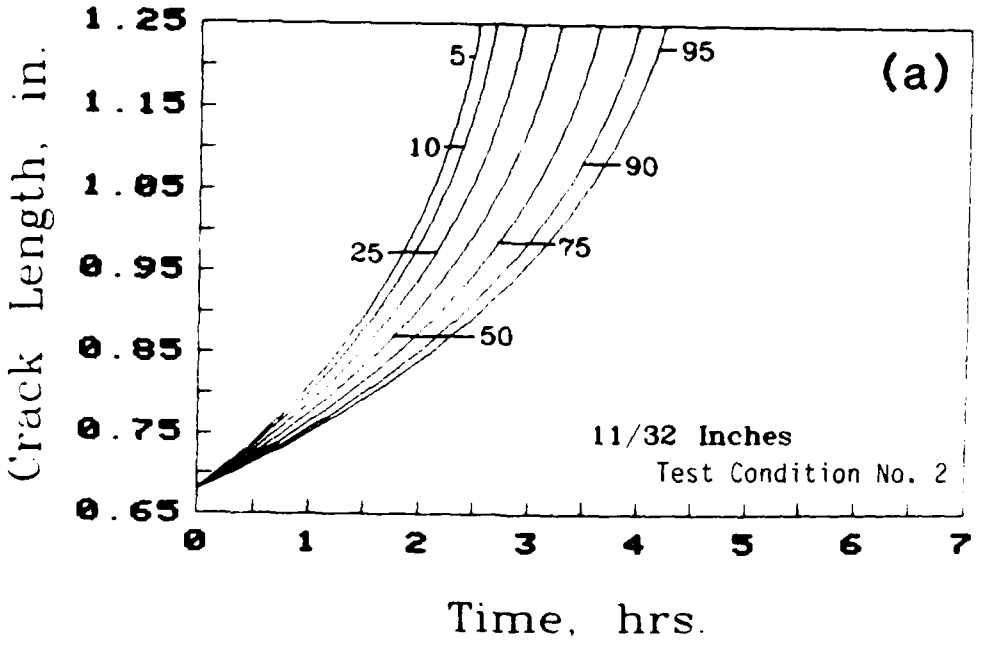

Figure 14(a). Crack Length a(t) Versus Time t for 11/32 Inches Thickness Group; Statistical Model.

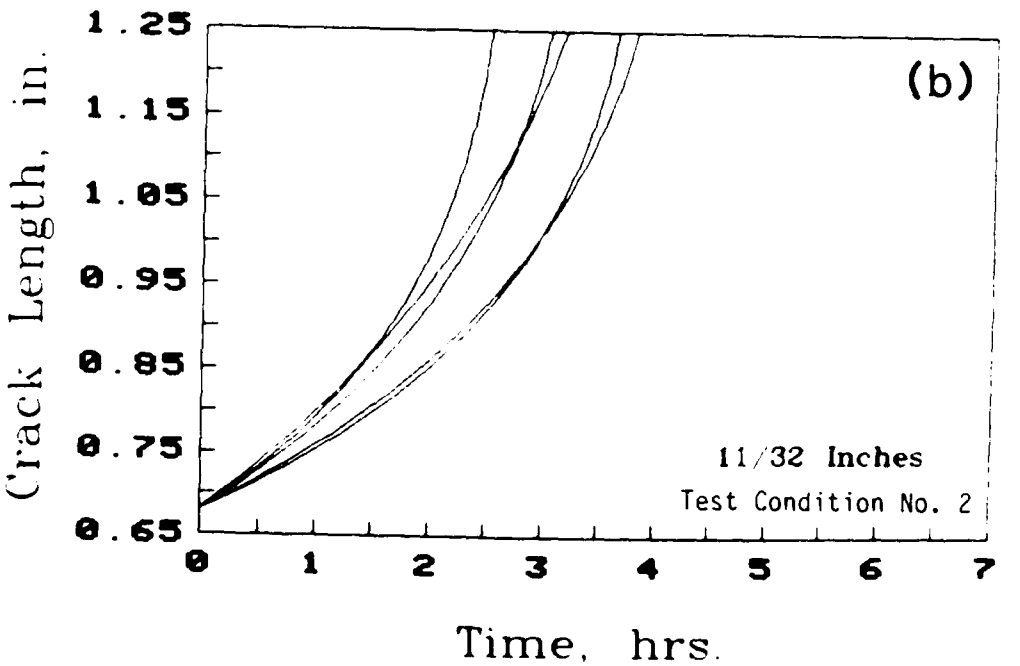

Figure 14(b). Crack Length a(t) Versus Time t for 11/32 Inches Thickness Group; Extrapolated Test Results.

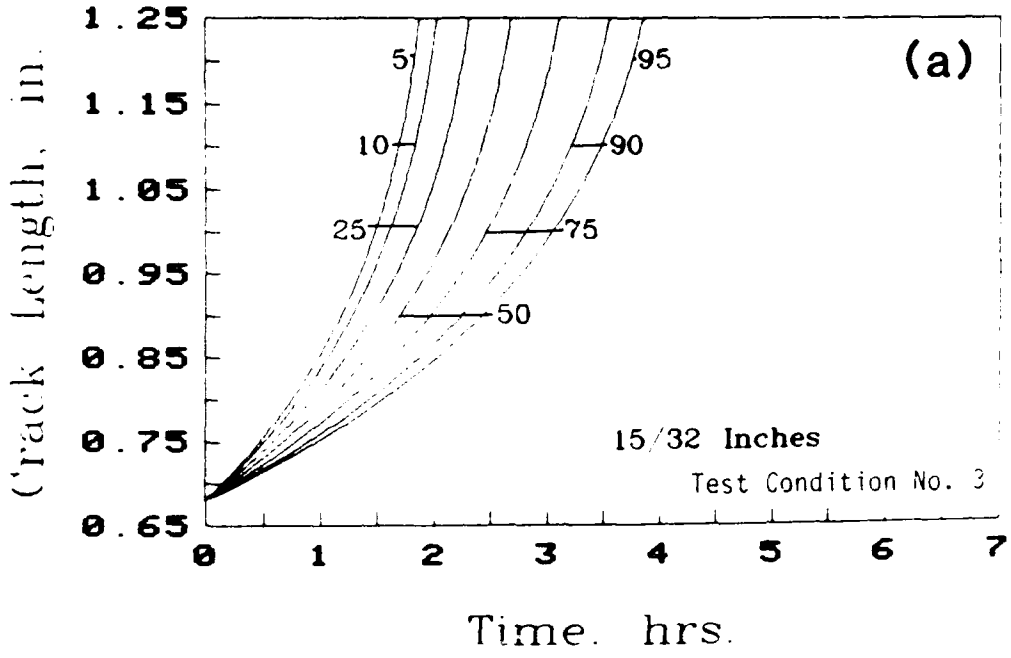

Figure 15(a). Crack Length a(t) Versus Time t for 15/32 Inches Thickness Group; Extrapolated Test Results.

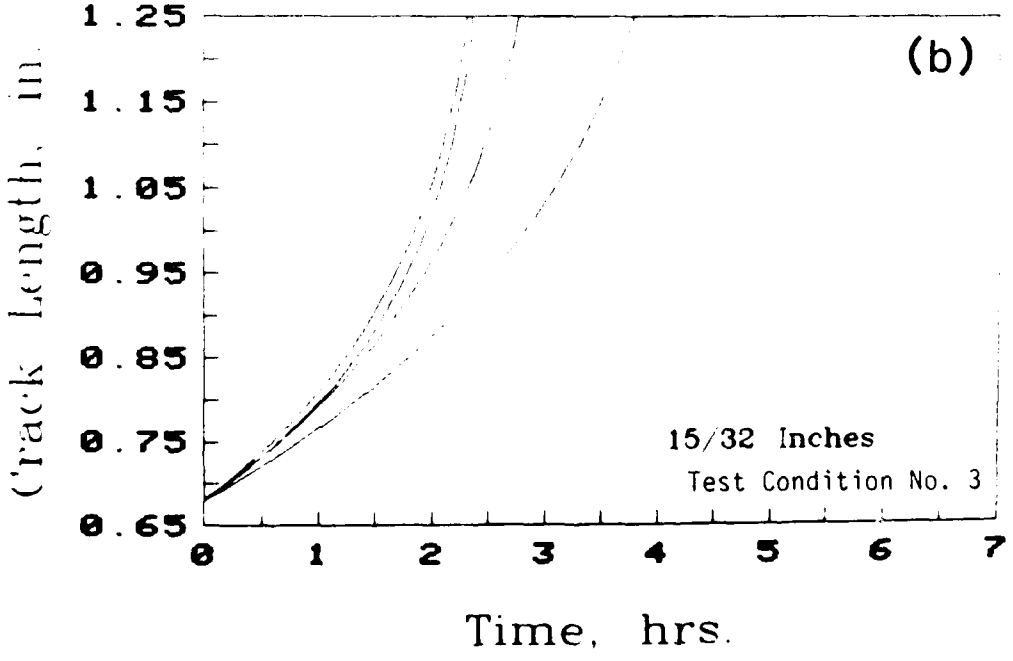

Figure 15(b). Crack Length a(t) Versus Time t for 15/32 Inches Thickness Group; Extrapolated Test Results.

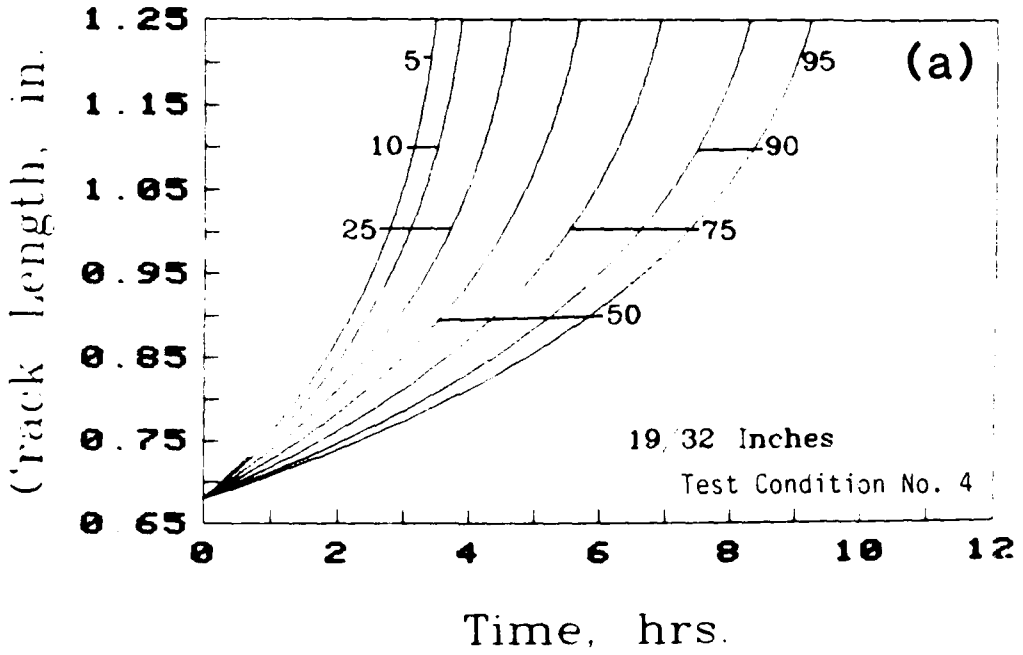

Figure 16(a). Crack Length a(t) Versus Time t for 19/32 Inches Thickness Group; Statistical Model.

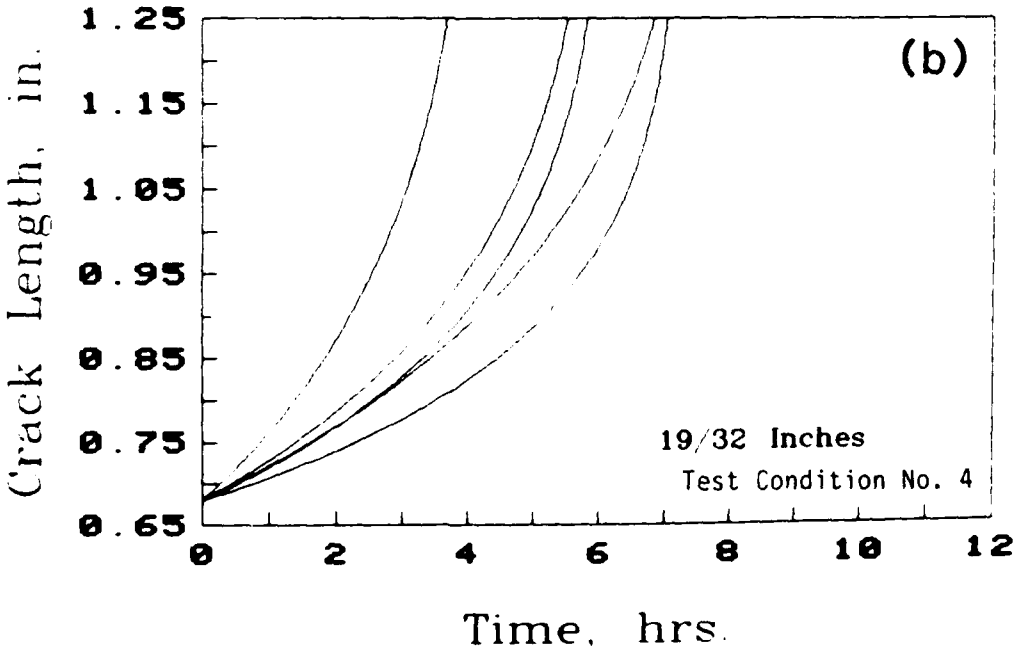

Figure 16(b). Crack Length a(t) Versus Time t for 19/32 Inches Thickness Group; Extrapolated Test Results.

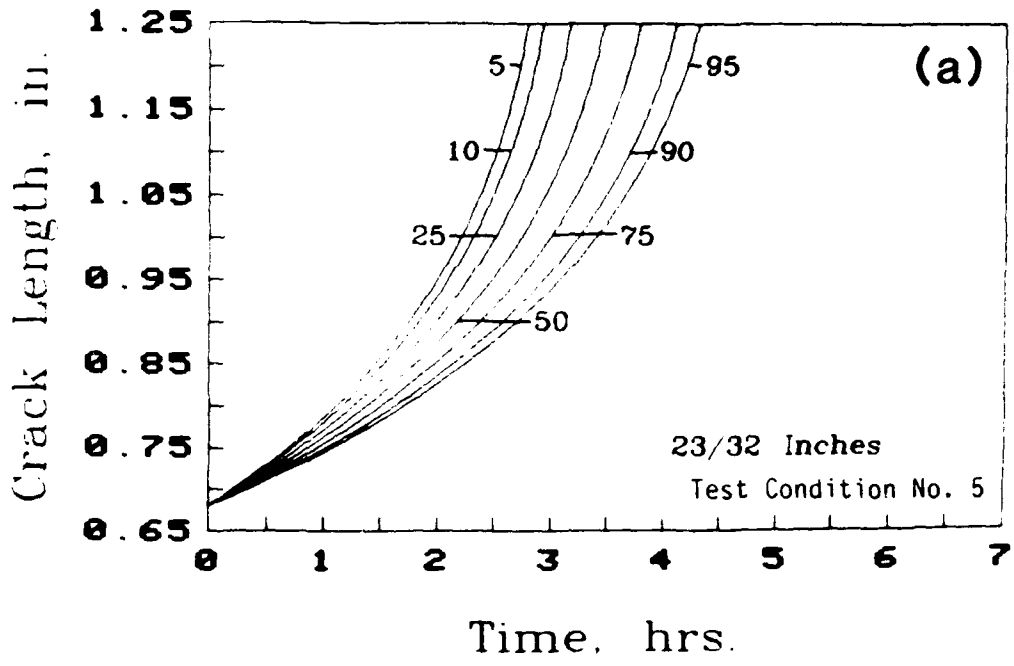

Figure 17(a). Crack Length a(t) Versus Time t for 23/32 Inches Thickness Group; Statistical Model.

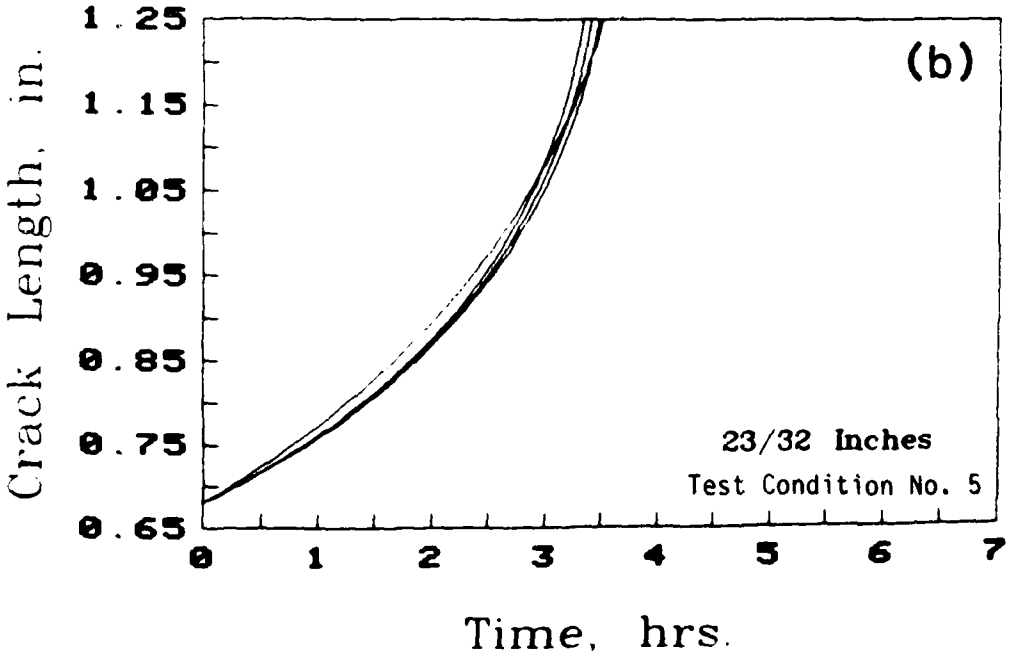

Figure 17(b). Crack Length a(t) Versus Time t for 23/32 Inches Thickness Group; Extrapolated Test Results.

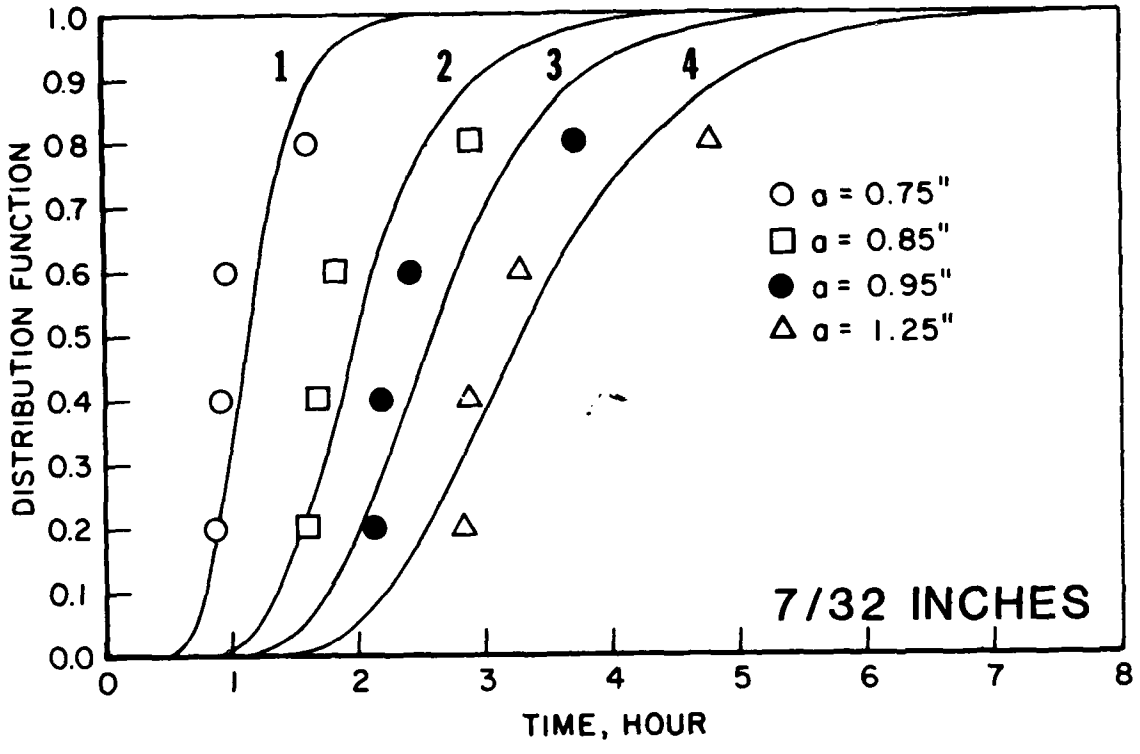

Figure 18. Correlation for Distribution of Time to Reach Given Crack Length for 7/32 Inches Thickness Group; Solid Curves for Statistical Model and ○ □ ● △ for Extrapolated Test Results.

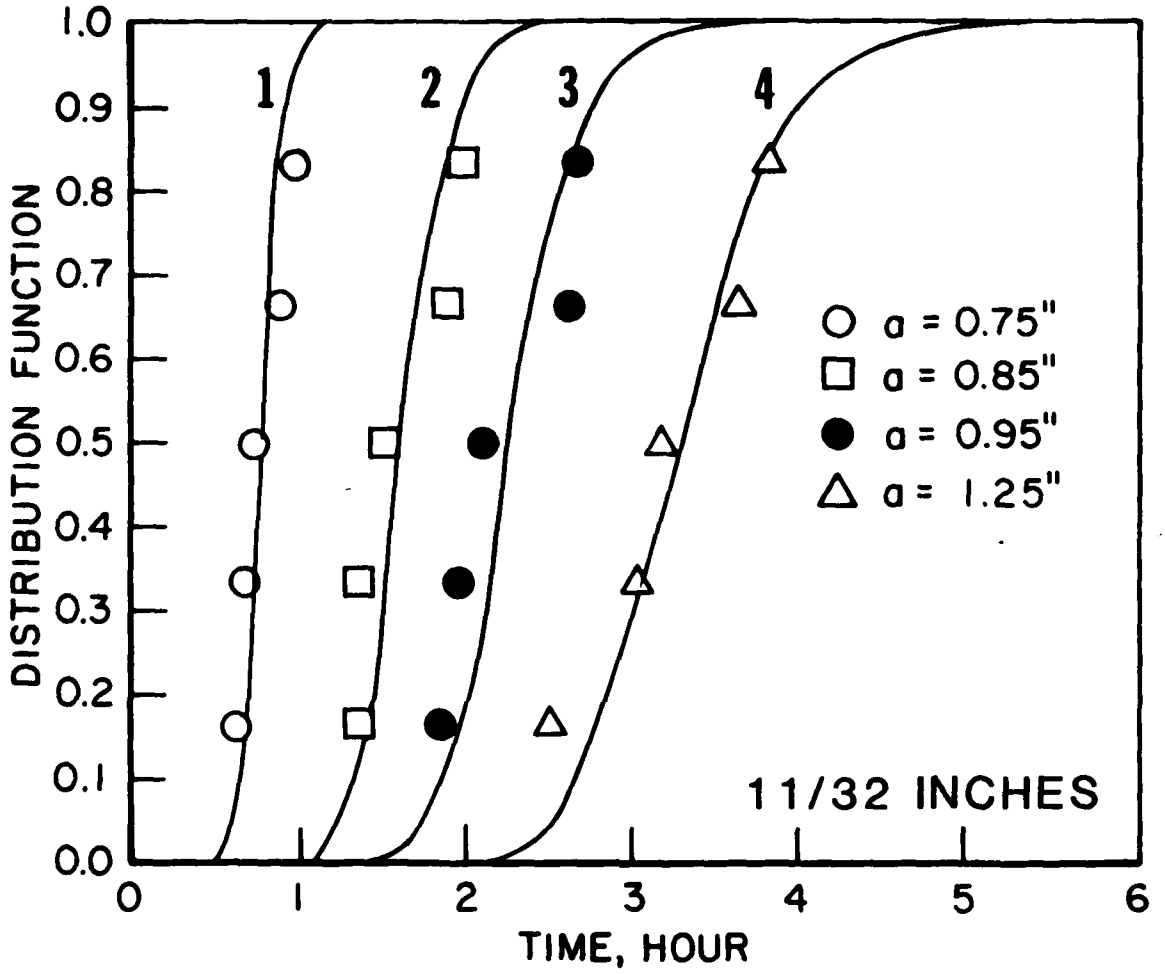

Figure 19. Correlation for Distribution of Time to Reach Given Crack Length for 11/32 Inches Thickness Group; Solid Curves for Statistical Model and ○ □ ● △ for Extrapolated Test Results.

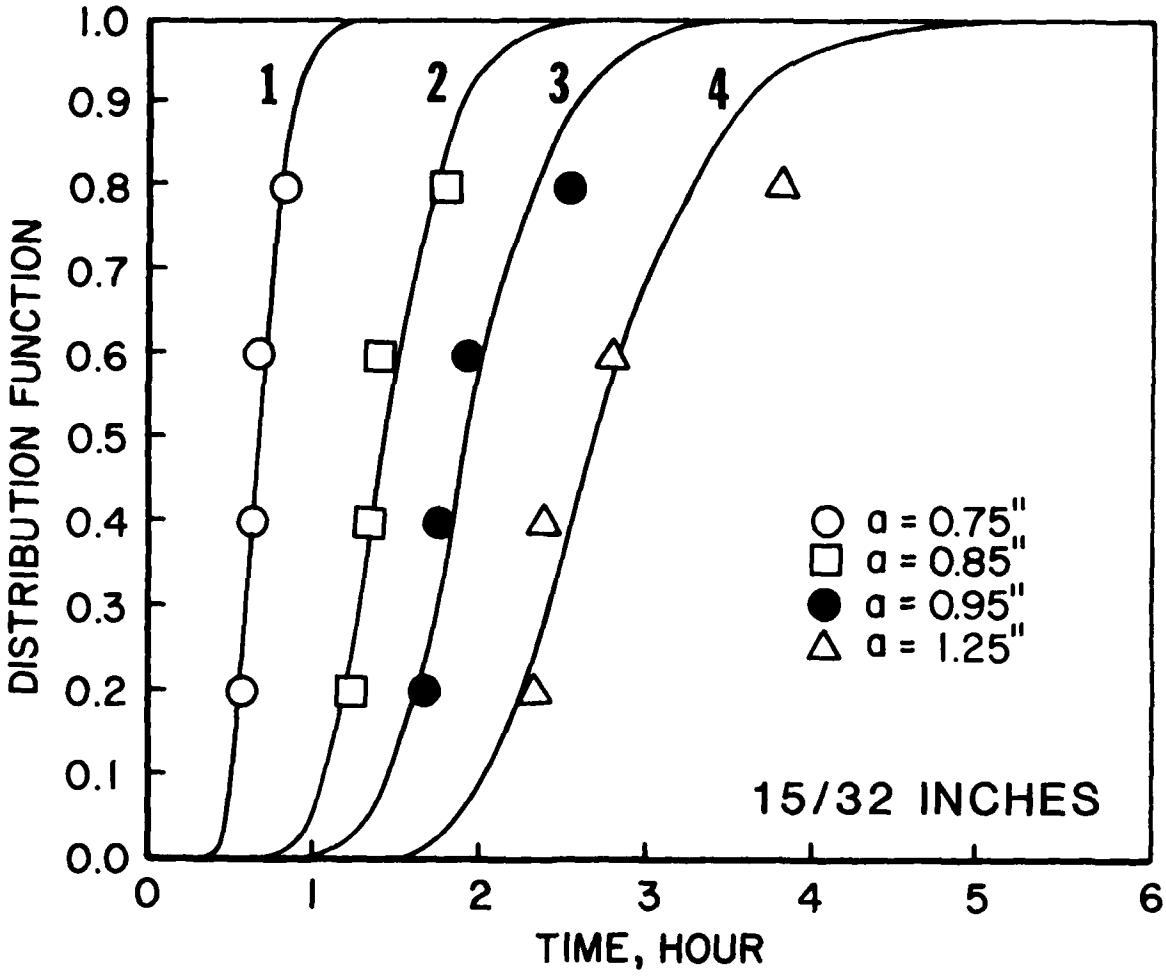

Figure 20. Correlation for Distribution of Time to Reach Given Crack Length for 15/32 Inches Thickness Group; Solid Curves for Statistical Model and ○ □ ● △ for Extrapolated Test Results.

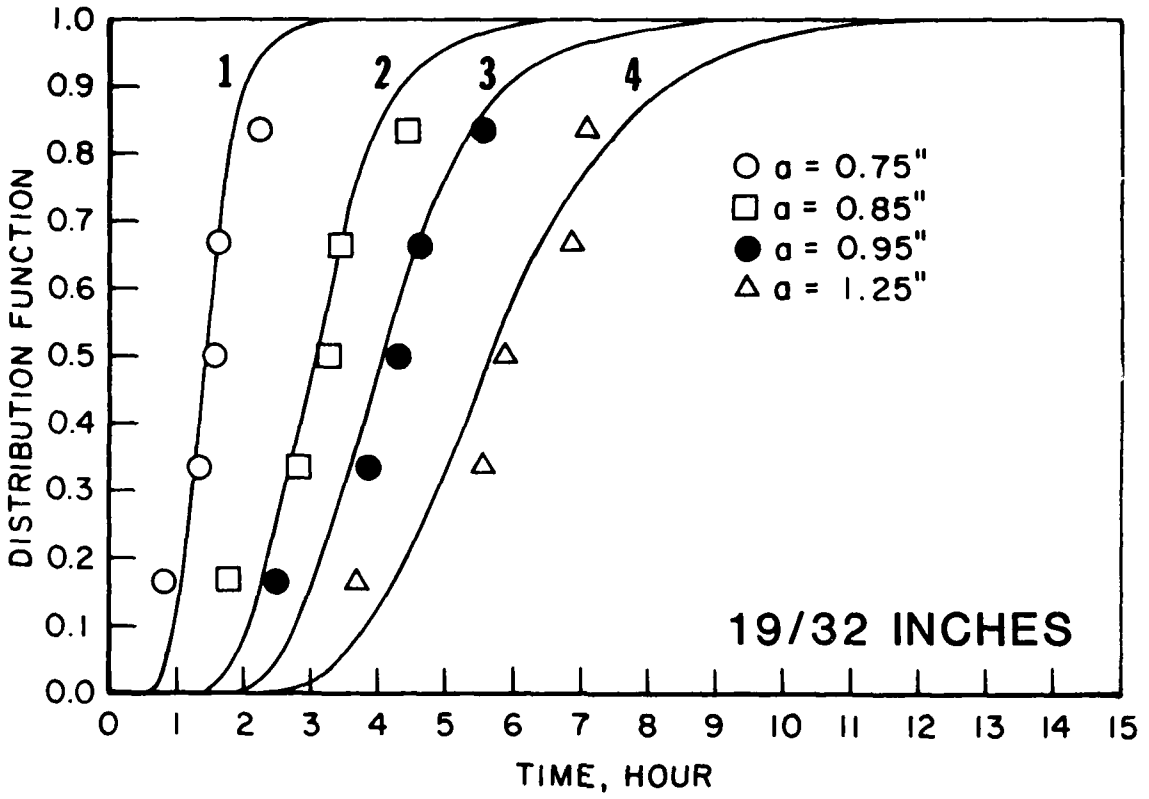

Figure 21. Correlation for Distribution of Time to Reach Given Crack Length for 19/32 Inches Thickness Group; Solid Curves for Statistical Model and ○ □ ● △ for Extrapolated Test Results.

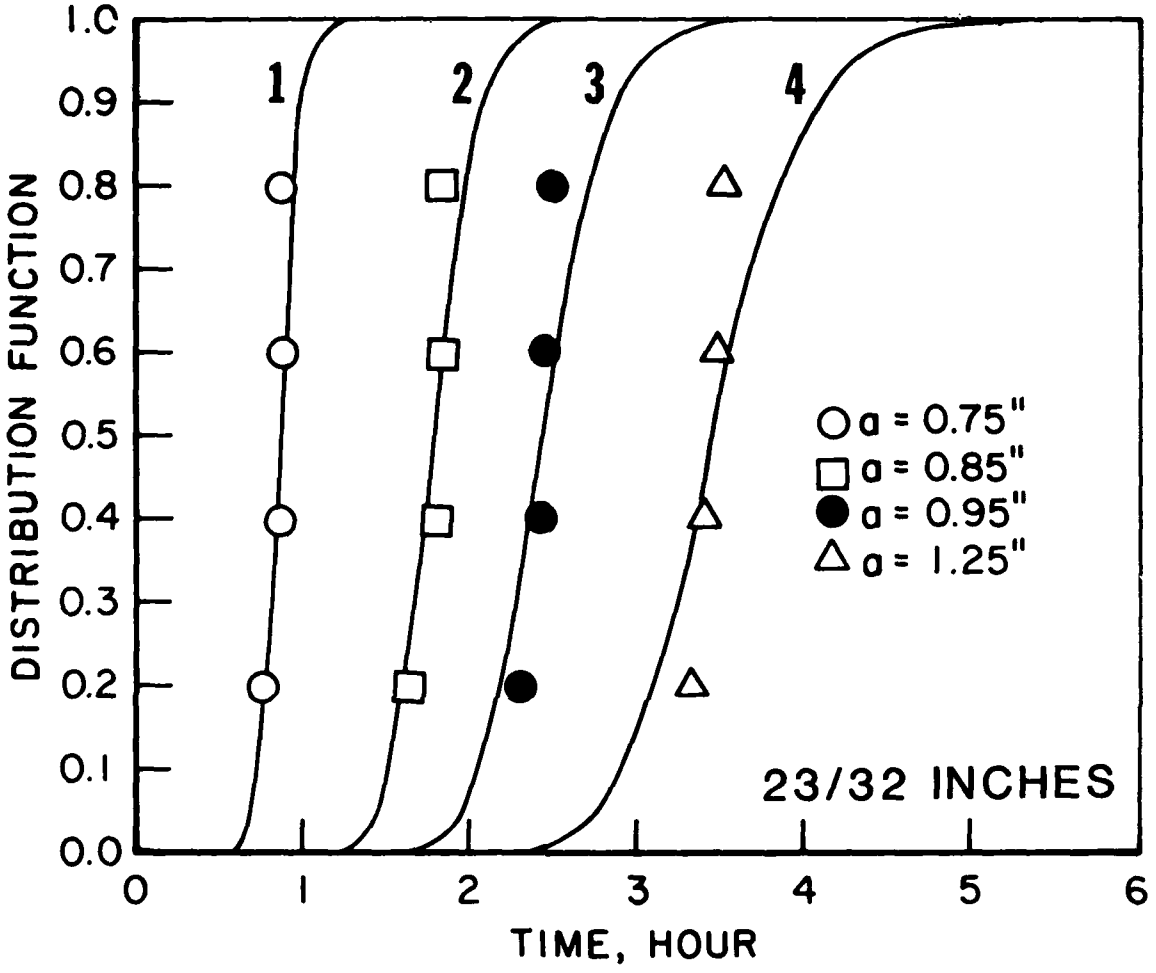

Figure 22. Correlation for Distribution of Time to Reach Given Crack Length for 23/32 Inches Thickness Group; Solid Curves for Statistical Model and ○ □ ● △ for Extrapolated Test Results.

The crack exceedance curves at different time instants, t, are obtained from Figures 13(a)-17(a) and plotted in Figures 23-27 as solid curves for the statistical model. For instance, a square shown on the solid curve in Figure 23 indicates that at t=1.5 hours, the probability that the crack length will exceed 0.8 inches (20.3 mm) (abscissa) is 0.4 (ordinate). The corresponding extrapolated test results are obtained from Figures 13(b)-17(b) by drawing a vertical line through the time of interest and the results are displayed in Figures 23-27 as circles. As expected, the exceedance probability reduces as the crack length increases. Again, the correlation for the crack exceedance curves between the statistical model and the extrapolated test results is very reasonable.

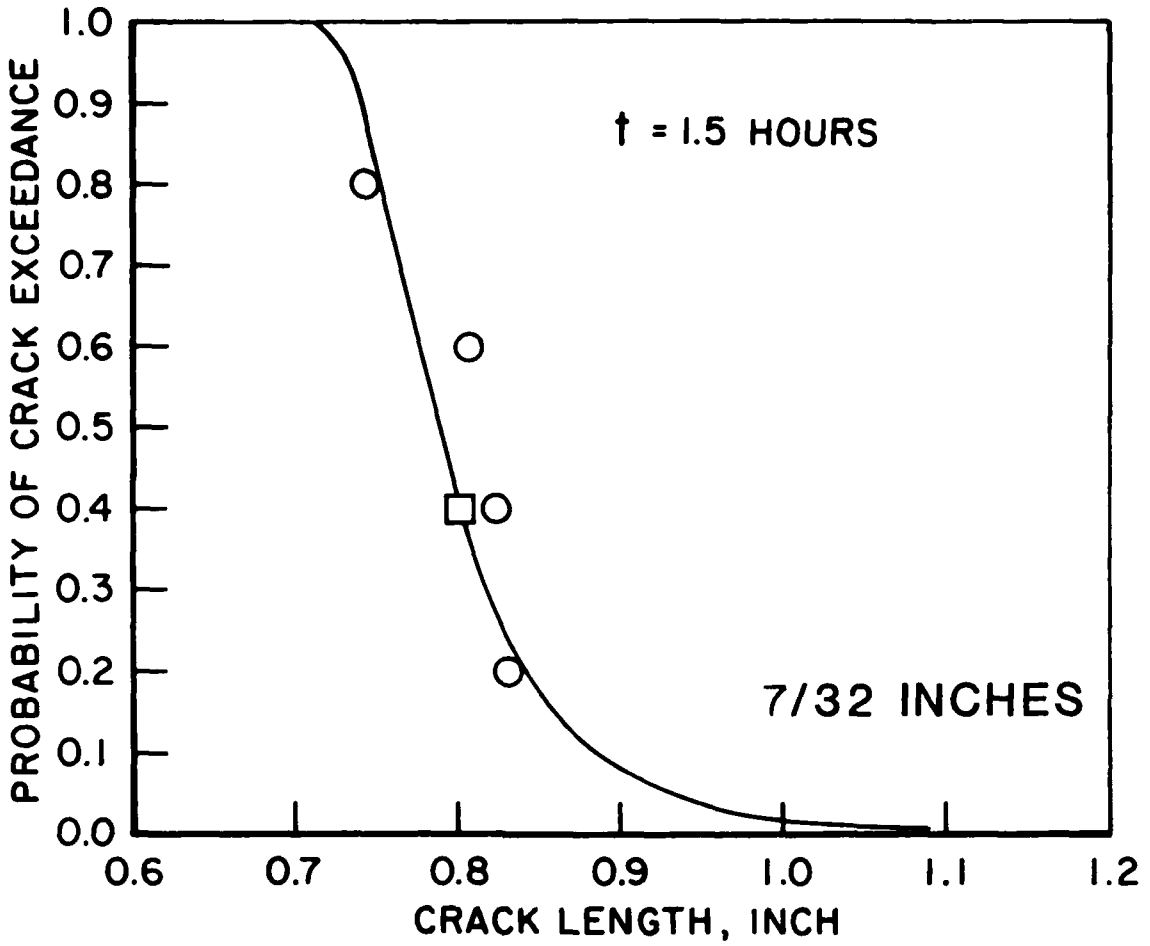

Figure 23. Probability of Crack Exceedance at t=1.5 Hours for 7/32 Inches Thickness Group; Solid Curve for Statistical Model and O for x Extrapolated Test Results.

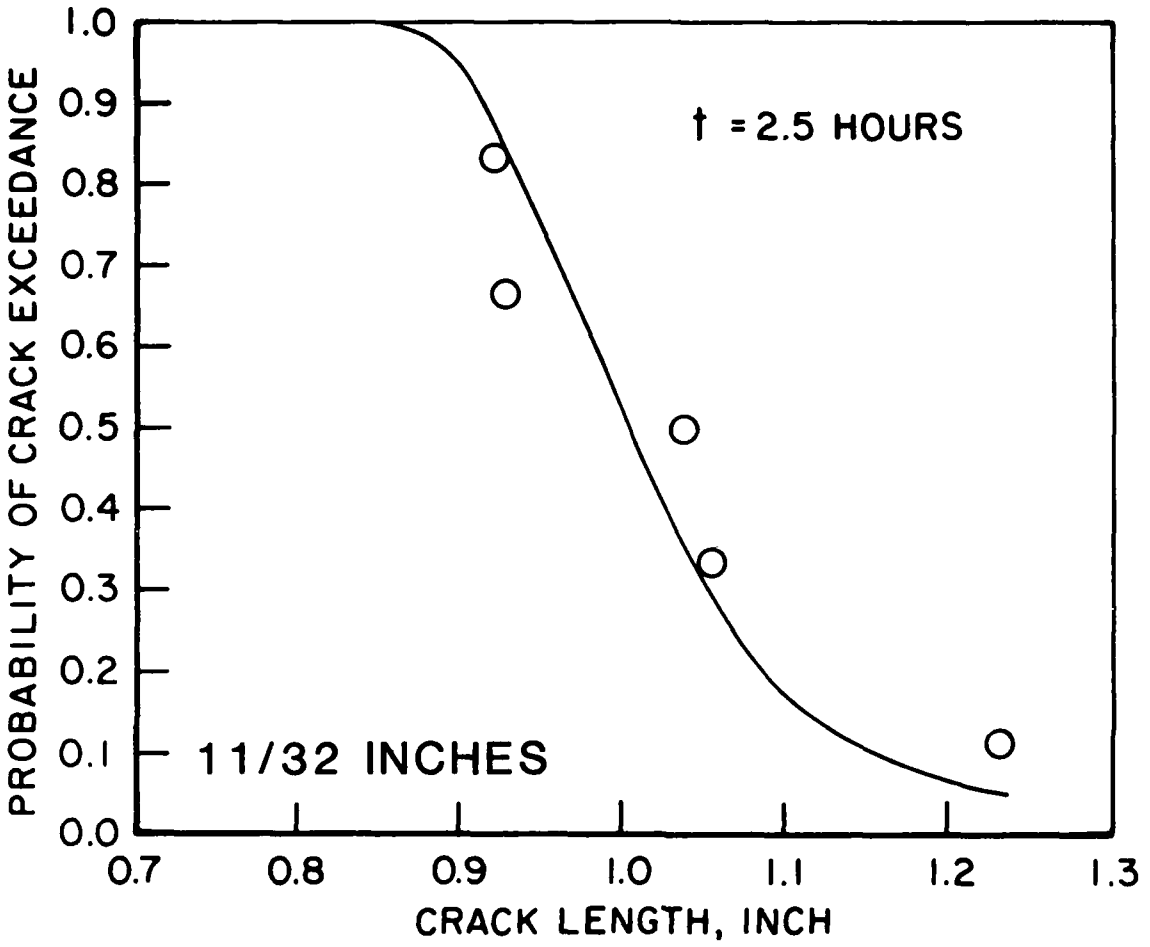

Figure 24. Probability of Crack Exceedance at t=2.5 Hours for 11/32 Inches Thickness Group; Solid Curve for Statistical Model and O for Extrapolated Test Results.

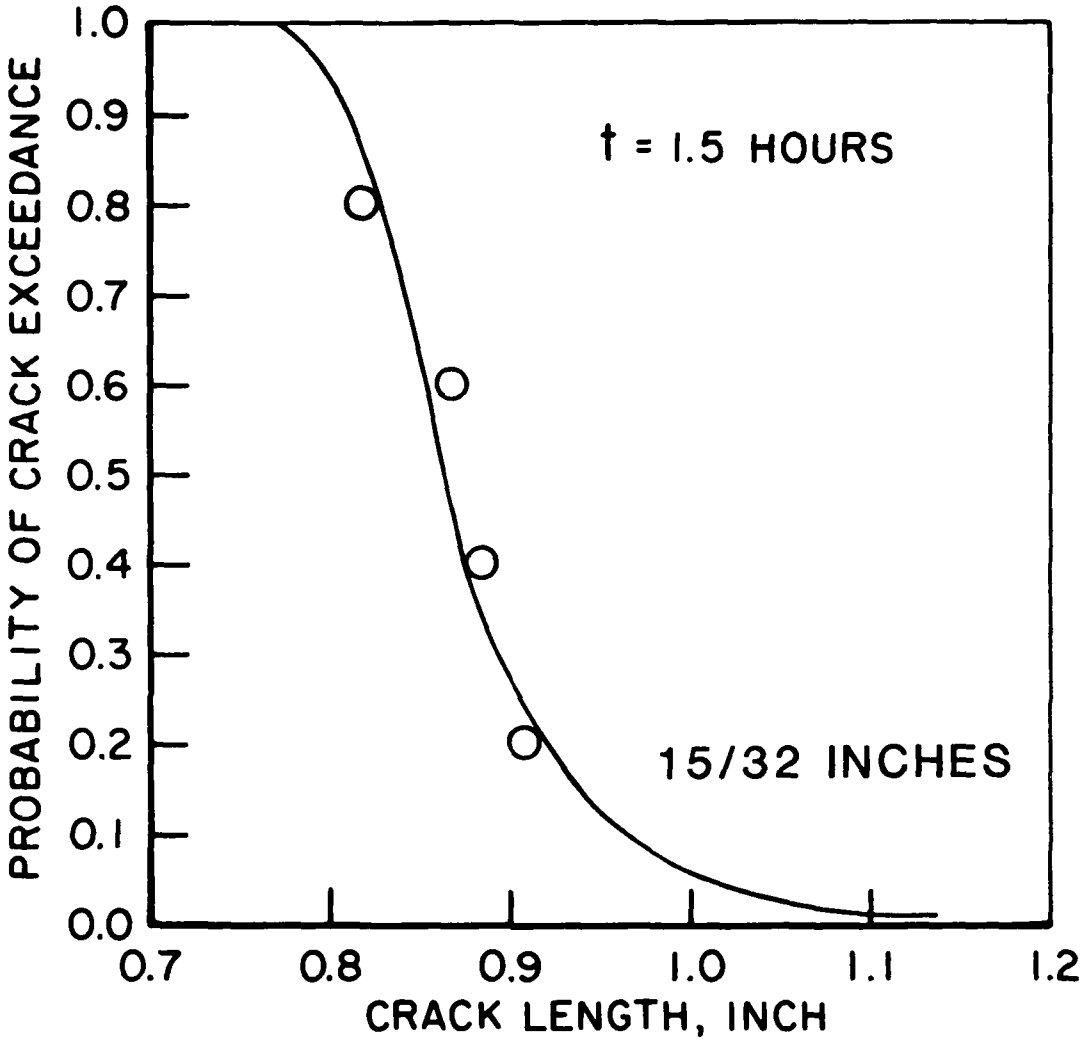

Figure 25. Probability of Crack Exceedance at t=1.5 Hours for 15/32 Inches Thickness Group; Solid Curve for Statistical Model and O for Extrapolated Test Results.

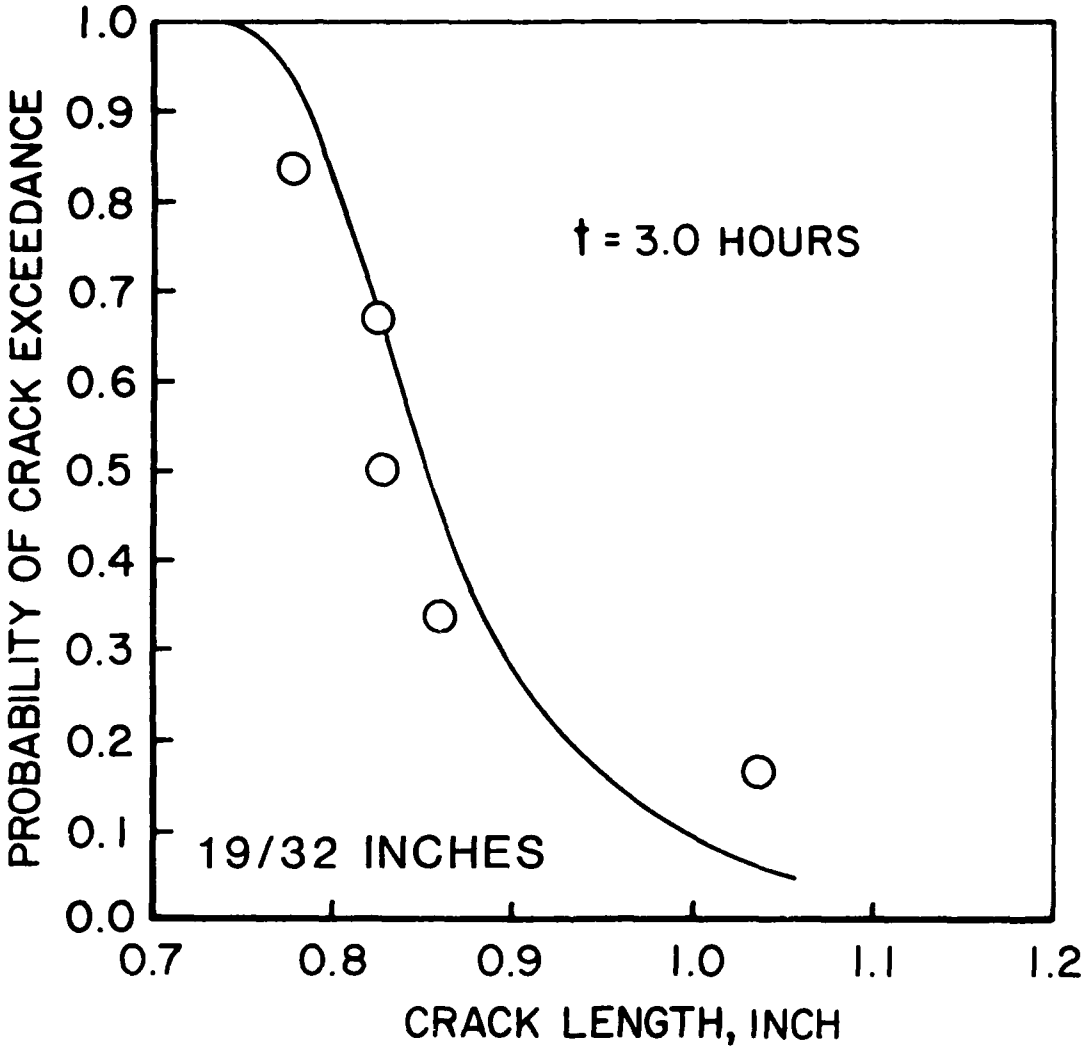

Figure 26. Probability of Crack Exceedance at t=3.0 Hours for 19/32 Inches Thickness Group; Solid Curve for Statistical Model and O for Extrapolated Test Results.

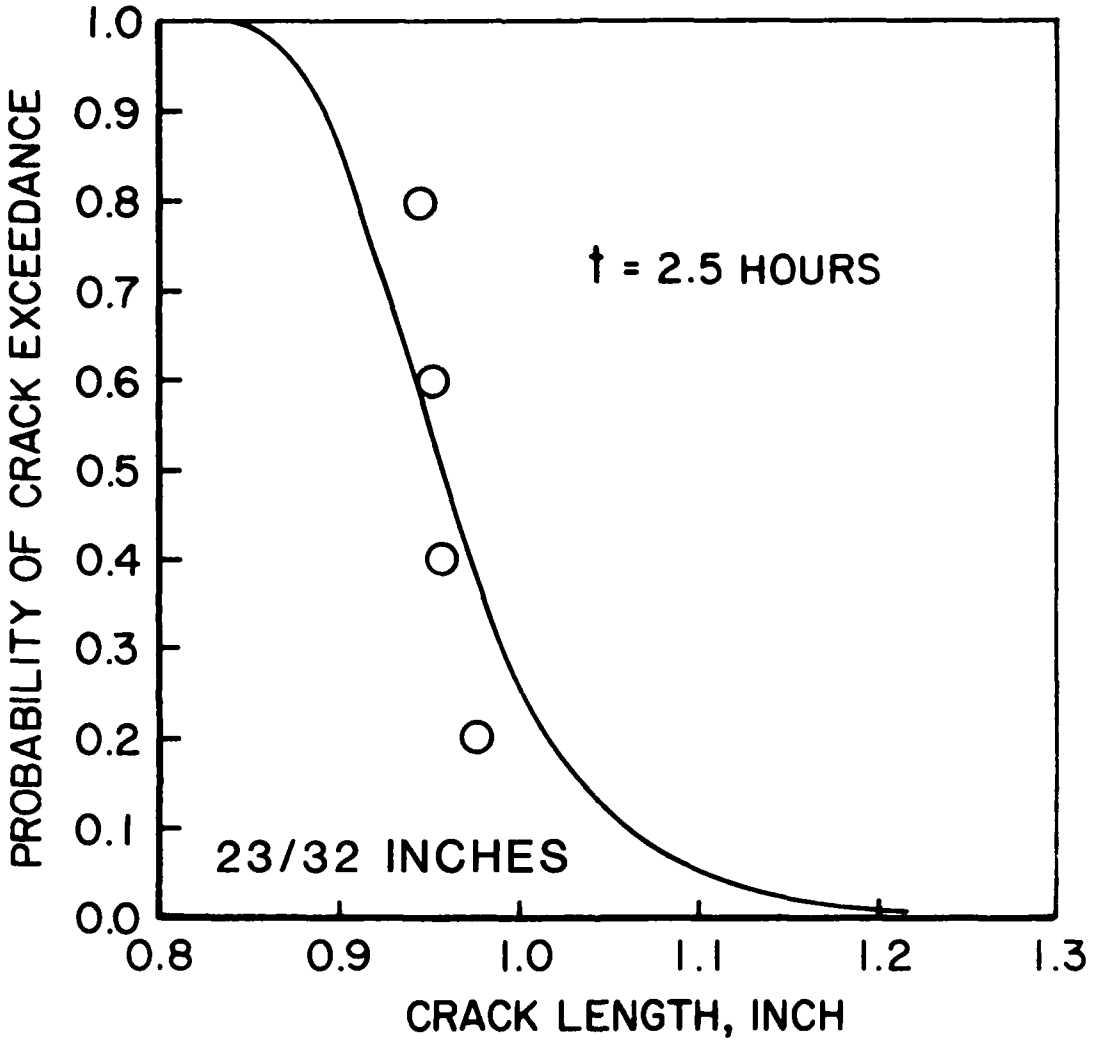

Figure 27. Probability of Crack Exceedance at t=2.5 Hours for 23/32 Inches Thickness Group; Solid Curve for Statistical Model and O for Extrapolated Test Results.

SECTION IV

CONCLUSIONS

A fracture mechanics-based statistical model for the crack growth behavior of engine materials under sustained loads at elevated temperature has been proposed and applied to the test results of IN100, a superalloy used in F100 engine disks. The method of maximum likelihood has been employed to calibrate the fracture mechanics parameters and the statistics of the model from the test results of the crack growth rate alone without using the data of crack length versus time. A correlation study is performed for the distribution of the crack length as a function of time, the distribution of time to reach any crack length, and the distribution of the crack length at any time. A good correlation has been demonstrated between the statistical model and the test results.

In view of the limited experimental test results presently available, the present statistical model is quite practical. This is because the maximum likelihood estimates of a few fracture mechanics parameters and the statistics of the model require neither a large number of test specimens nor a homogeneous data base for crack length versus time.

REFERENCES

1. R.C. Donath, T. Nicholas, and L.S. Fu, "An Experimental Investigation of Creep Crack Growth in IN100," Fracture Mechanics: Thirteenth Conference, ASTM STP 743, Richard Roberts, Ed., America Society in Testing and Materials, 1981, pp. 186-206.

2. R.C. Donath, Crack Growth Behavior of Alloy IN100 Under Sustained Load at 732°C (1350°F), Technical Report AFWAL-TR-80-4131, April 1981, Wright-Patterson Air Force Base, Ohio 45433.

3. J.M. Larson, B.J. Schwartz, and C.G. Annis, Jr., Cumulative Fracture Mechanics Under Engine Spectra, Technical Report AFML-TR-79-4159, Wright-Patterson Air Force Base, 1980.

4. J.N. Yang, G.C. Salivar, and C.G. Annis, Jr., Statistics of Crack Growth in Engine Materials; Vol. 1: Constant Amplitude Fatigue at Elevated Temperature, Technical Report AFML-TR-82-4040, Wright-Patterson Air Force Base, 1982.

5. J.N. Yang, G.C. Salivar, and C.G. Annis, Jr., "Statistical Modeling of Fatigue Crack Growth in a Nickel-Base Superalloy," paper to appear in the Journal of Engineering Fracture Mechanics, 1982.

6. Y.K. Lin and J.N. Yang, "On Statistical Moment of Fatigue Crack Propagation," paper to appear in the Journal of Engineering Fracture Mechanics, 1982.